INVESTIGATING THE MECHANISMS RESPONSIBLE FOR CEPHALOSPORIN RESISTANCE IN *CLOSTRIDIOIDES DIFFICILE* STRAIN 630

By

Lara Anna Turello

Bachelor of Science – Biological Sciences
University of Nevada, Las Vegas
2016

A thesis submitted in partial fulfillment
of the requirements for the

Master of Science – Biochemistry

Department of Chemistry and Biochemistry
College of Sciences
The Graduate College

University of Nevada, Las Vegas
May 2020

UNLV | GRADUATE COLLEGE

Thesis Approval

The Graduate College
The University of Nevada, Las Vegas

May 15, 2020

This thesis prepared by

Lara Anna Turello

entitled

Investigating the Mechanisms Responsible for Cephalosporin Resistance in *Clostridioides difficile* Strain 630

is approved in partial fulfillment of the requirements for the degree of

Master of Science – Biochemistry
Department of Chemistry and Biochemistry

Ernesto Abel-Santos, Ph.D.
Examination Committee Chair

Kathryn Hausbeck Korgan, Ph.D.
Graduate College Dean

Gary Kleiger, Ph.D.
Examination Committee Member

Ronald Gary, Ph.D.
Examination Committee Member

Brian Hedlund, Ph.D.
Examination Committee Member

Jeffery Shen, Ph.D.
Graduate College Faculty Representative

ABSTRACT

Clostridioides difficile infection (CDI) is one of the most common nosocomial infections worldwide. A major risk factor for CDI is antibiotic therapy, due to C. *difficile*'s resistance to a myriad of antibiotics—one of which are cephalosporins. Cephalosporins are ß-lactam antibiotics that function by binding to the active site of penicillin-binding proteins (PBPs), thus inhibiting peptidoglycan synthesis and leading to cell lysis. Gram-positive bacteria can counteract ß-lactams by (i) producing ß-lactamases, (ii) expressing modified PBPs, or (iii) by expressing efflux pumps.

Genomic analysis of *C. difficile* strain 630 revealed the presence of at least 31 putative ß-lactam resistance genes that encode putative ß-lactamases, ß-lactamase-like proteins and PBPs. We hypothesized that upon cephalosporin exposure, *C. difficile* would differentially express one or more of these genes. Many of these genes were differentially expressed when *C. difficile* was exposed to cefoxitin, but most of them were not upregulated more than 3.5-fold according to RT-qPCR analysis. Strikingly, putative ß-lactamase, *blaCDD*, was upregulated nearly 600-fold upon cefoxitin treatment. Deletion of *blaCDD* caused little to no reduction in cephalosporin resistance. RT-qPCR analysis of the *blaCDD*-null mutant when treated with cefoxitin did not reveal any drastic changes in expression of the remaining genes that could explain transcription compensation for the deleted ß-lactamase. Deletion of the second-most upregulated gene which encodes a putative PBP, *vanY*, minimally affected cephalosporin resistance.

To elucidate additional putative resistance genes that may be differentially regulated upon cephalosporin exposure, we analyzed the entire *C. difficile* transcriptome using RNA-Seq. We found that upon cephradine, ceftazidime, and cefepime treatment, expression was similar to untreated cells. Cefoxitin-treated cells, however, had a higher number of differentially regulated

genes. This might be attributed to the activation of starvation responses due to longer treatment time for cefoxitin-treated cells. Nevertheless, all cephalosporin treatments triggered the upregulation of a putative heterodimeric ABC transporter directly downstream of *blaCDD*. Further functional analysis of this ABC transporter will be necessary to elucidate its possible role in cephalosporin resistance. Future studies will be geared towards using transposon mutagenesis to elucidate genes that are required for *C. difficile*'s survival upon cephalosporin treatment but that are constitutively expressed regardless of antibiotic exposure.

ACKNOWLEDGEMENTS

These past three years have been the most challenging, emotionally-taxing, yet rewarding journey I have experienced in my academic career. Despite the seemingly endless struggles, I persevered due the overwhelming support I have received from the family, friends, and colleagues around me.

I would first like to give my deepest thanks to my advisor, Dr. Ernesto Abel-Santos, for his unwavering support and steady guidance, even when I thought there was no end in sight. You taught me to be more independent and think critically about my work, characteristics that will be integral in my career. But most importantly, you taught me to believe in myself as a capable scientist.

Thank you to my graduate committee members, Dr. Gary Kleiger, Dr. Ronald Gary, Dr. Brian Hedlund, and Dr. Jeffery Shen. I never felt intimidated to approach any of you whenever I had questions or concerns during my research. Every one of you has given me valuable insight in how to proceed with my work.

Thank you to the Dr. Edwin Oh Lab at the Nevada Institute of Personalized Medicine for their help and collaboration in obtaining and analyzing the RNA-Seq data in this thesis. Also, thank you to Cale Seymour for his integral work on visualizing the RNA-Seq data, as well.

I also give a heartfelt thanks to the entire Abel-Santos Squad. From day one in the lab, I felt included, supported, and respected by everyone. We are truly a lab family. A special thanks to Dr. Christopher Yip and Amber Consul, who were especially involved in helping me complete this work. Chris, thank you for training me, helping me with experiments, and letting me shower you with questions day in and day out; I feel like I gained not only a great colleague, but a great friend, as well. Amber, thank you for the immense hands-on work you were involved with in

this thesis, as well as being an incredibly genuine and understanding friend when I was at my lowest. You really pepped me up when I was down. I would also like to thank Dr. Israel Alvarado. Israel, you were someone who I could always turn to when I was struggling through developing my qPCR assays; thank you for always responding to my countless emails with insightful suggestions. Thank you to the undergraduate assistants who also helped ease some of the hands-on demand for some of these experiments.

I would like to thank my mother for always listening to my hardships and bouts of self-doubt during the past three years. Thank you for encouraging me to keep pursuing this challenging career I have chosen. (Insert sarcastic tone) I know how "utterly devasted" you were when I decided not to pursue music…

I would also like to thank my father for being one of the reasons I even gained an interest in the sciences. *Grazie papà, per avermi sostenuta, anche a distanza.*

Lastly, but certainly not least, I would like to thank my partner, O.J. My love, you have been my rock, my cheerleader, and my personal therapist throughout all of this. Honestly, I do not know how you kept sane listening to my worries and stresses almost every day. Thank you for pushing me to keep going even though I felt like I would never finish.

DEDICATION

This thesis is dedicated to Mariella Maranzana and Sebastiano Buda, who have always served as grandparents to me rather than my great-aunt and -uncle. They have always loved me and supported me unconditionally. *Grazie per essermi stati vicini, anche se fisicamente lontani. Vi voglio un mondo di bene.*

TABLE OF CONTENTS

LIST OF TABLES

LIST OF FIGURES

LIST OF EQUATIONS

CHAPTER 1: Introduction

1.1 *Clostridioides difficile*

1.1.1 *Background and Significance*

Clostridioides (Clostridium) difficile is a motile, spore-forming anaerobic bacterium that was first isolated in 1935 from the stool of healthy new-born infants (1). At the time, it was named *Bacillus difficilis* because of its rod-like shape and the difficulty in its isolation and cultivation (1). Hall and O'Toole also reported that this new bacterium likely produced a "soluble exotoxin" that could cause bowel edema in guinea pigs and rabbits, as well as convulsions in guinea pigs when broth culture filtrate was injected subcutaneously. It was later discovered that *C. difficile* can produce two main toxins (TcdA and TcdB) that target Ras family GTPases (2–4). Though *C. difficile* was known to produce toxins that affected animals, it was not until 1978 that *C. difficile* was found to cause disease in humans (5). Bartlett *et al*. collected stool samples from patients who had undergone antibiotic therapy prior to *Clostridioides difficile* infection (CDI) onset (5). This suggested a key characteristic of CDI: it is an antibiotic-associated infection.

C. difficile is resistant to a myriad of antibiotics including fluoroquinolones and cephalosporins (6, 7), allowing the pathogen to flourish and cause infection in the gut of patients undergoing antibiotic therapy. Over the decades, this characteristic has in part enabled CDI to become the most common hospital-acquired infection (HAI) in the United States (8). In 2011, there were approximately 500,000 CDI incidences nationwide (9). Over 29,000 of those incidences lead to death within the first 30 days after the initial diagnosis (9). In 2014, hospitalization of CDI patients costed the US government $5.4 billion dollars in medical costs, posing an economic burdenas well (10). Though the 2019 report issued by the US Centers for

Disease Control and Prevention (CDC) reported a decrease in hospital-acquired CDI incidents, *C. difficile* is still considered an urgent threat (11). Further investigating the mechanisms involved in this pathogen's virulence is crucial in preventing the propagation of antibiotic resistance.

1.1.2 *Taxonomic Classification*

Clostridioides difficile is a Gram-positive, spore-forming obligate anaerobe (**Figure 1.1**). *C. difficile* is a part of the *Firmicutes* phylum, which comprises of mostly Gram-positive, endospore-forming bacteria that have low G-C content (12). This phylum is divided into five classes: *Bacilli*, *Clostridia*, *Erysipelotrichia*, *Negativicutes*, and *Thermolithobacteria* (12). *C. difficile* falls under the *Clostridia* class, which includes strict anaerobes (13). Finally, *C. difficile* is a member of the *Clostridiales* order and *Peptostreptococcaceae* family.

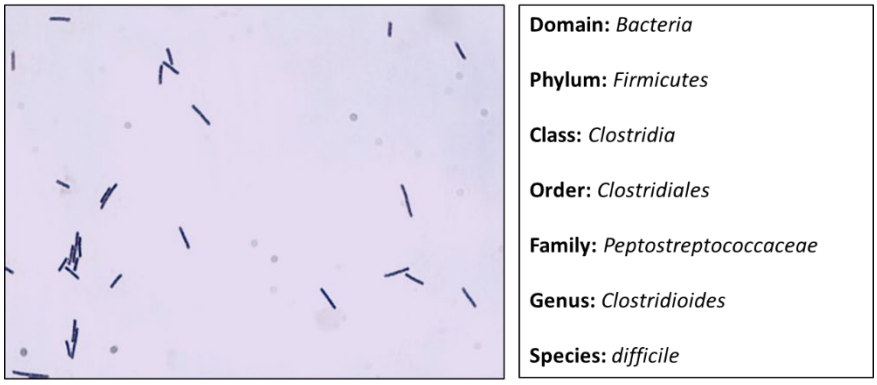

Figure 1.1. *Clostridioides difficile* Gram-stain and taxonomic classification. (Left) Gram-stain of *C. difficile* strain 630 vegetative cells. (Right) Taxonomy of *C. difficile*.

The genus of the bacterium recently changed from *Clostridium* to *Clostridioides* (14) due to restriction of the former genus (15). Briefly, 16S rRNA sequencing studies revealed the

heterogeneity in *Clostridium* species (15). It was proposed that the genus be constricted to species that are a part of the phylogenetic cluster containing the *Clostridium* type strain, *Clostridium butyricum* (15). *C. difficile* falls outside of this cluster (15). Thus, it was proposed to reclassify *C. difficile* using a novel genus, *Clostridioides—C. difficile* being the type strain (14). To date, *C. difficile* is the only other member of the *Clostridioides* genus along with *Clostridioides mangenotii* (14). Despite the genus *Clostridium* still being acceptable nomenclature for this bacterium (16), the genus used for the remainder of this thesis will be *Clostridioides*.

1.1.3 Clostridioides difficile *Infection*

Clostridioides difficile infection (CDI) is dynamic and can range in its severity. Moderate symptoms include diarrhea, nausea, abdominal discomfort, and vomiting (17). Symptoms for severe cases include pseudomembranous colitis, bloody diarrhea, sepsis, and even death (17, 18).

Risk factors that may affect the severity of the infection are advanced age, immunodeficiency, and antibiotic therapy (17, 19–22). In 2011, individuals older than 65 years of age had a CDI incidence rate of 627.7 per 100,000 persons, whereas individuals between the ages of 45 and 64 had a more than four-fold lower CDI incidence rate of 148.5 per 100,000 persons (21). Regarding immunodeficiency, a study spanning data from 1992 to 2002 found that clinical AIDS patients had a CDI incidence rate ratio of 9.89 with respect to patients without AIDS (22).

Despite advanced age and immunodeficiency both increasing the risk of CDI onset, a majority of CDI incidences have a common prerequisite: antibiotic therapy. In fact, certain antibiotics have been commonly associated with CDI, like clindamycin, amoxicillin, ampicillin,

cephalosporins, and fluoroquinolones (17, 23–26). Second- and third-generation cephalosporin have been especially associated with hospital-acquired CDI (24). In a 2013 study, the odds ratio for worldwide hospital-acquired CDI incidence after the use of second-generation cephalosporins was 2.23, whereas the use of third-generation cephalosporins gave an odds ratio of 3.20 (24).

The infectious agents of CDI are *C. difficile* spores. Unlike *C. difficile* vegetative cells, the spores are dormant, oxygen tolerant, and resilient to several environmental factors. *C. difficile* vegetative cells undergo sporulation upon the presence of stressors like nutrient deprivation and dessication (27). Only in the right environmental conditions will spores germinate into toxin-producing vegetative cells. *C. difficile* spores germinate upon the binding of bile salts and amino acids to specific germination receptors (28). These environmental cues are especially abundant in the intestines of patients undergoing antibiotic treatment.
Individuals undergoing antibiotic therapy have a compromised gut microbiome. This dysbiosis in the natural gut microbial flora creates the ideal environment for *C. difficile* spores to germinate and colonize in the lower gastrointestinal tract, leading to infection (29). In the gut of healthy individuals, the microbial flora metabolizes *C. difficile* germinants (molecules triggering germination) such as bile salts produced by the liver, preventing the spores from germinating into toxin-producing vegetative cells (29). In individuals undergoing antibiotic therapy, the microbiome dysbiosis causes a depletion in the microbes involved in bile salt metabolism, allowing those bile salts to accumulate and trigger *C. difficile* spore germination (28, 29).

Furthermore, the major risk factor for CDI is antibiotic therapy because *C. difficile* is generally resistant to the very antibiotics used for the said therapy (**Figure 1.2**) (30). The disruption of the indigenous microbial flora upon antibiotic treatment increases the CDI risk caused by antibiotic-resistant *C. difficile*. Once the antibiotic therapy stops, the microbial flora is

still disrupted, now allowing antibiotic-susceptible *C. difficile* strains to cause infection. Only upon the restoration of the normal microbial flora does the risk of CDI vanish.

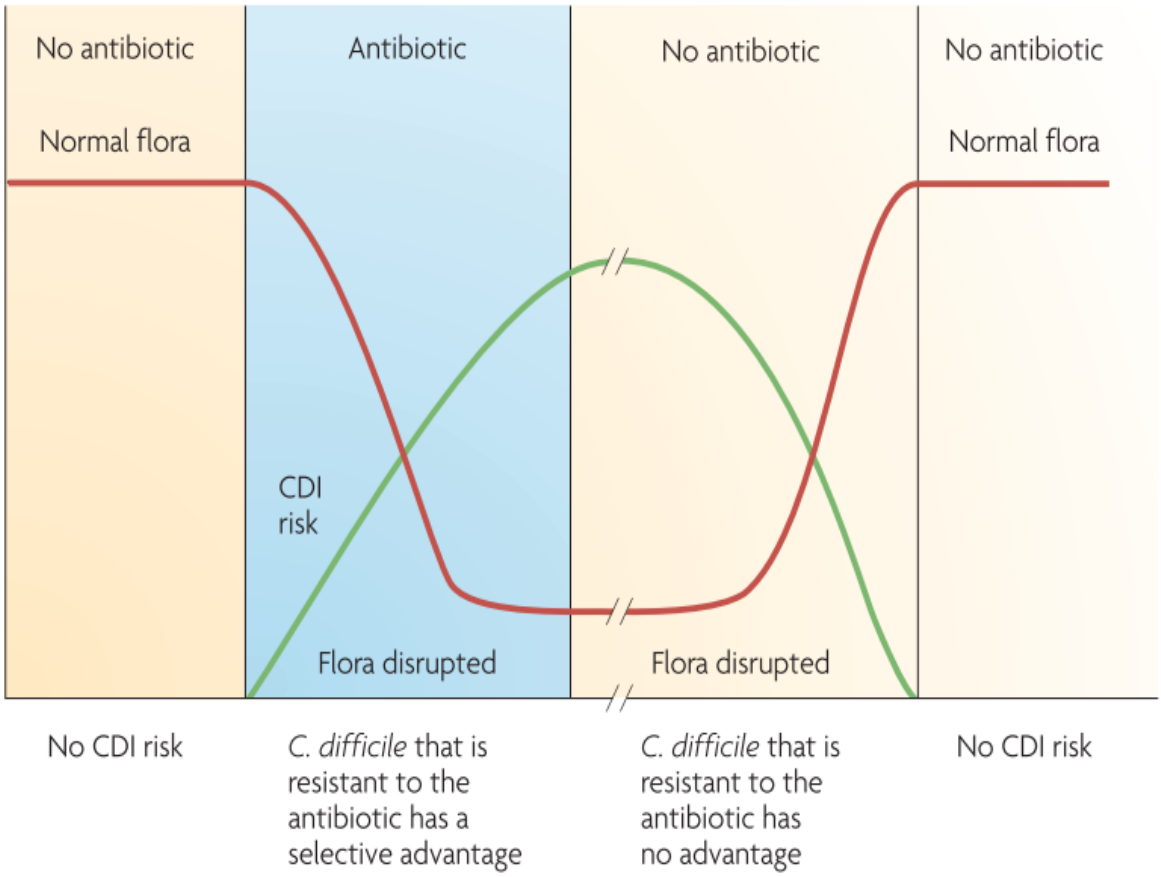

Figure 1.2. The risk of CDI onset in relation to the natural gut microbial flora and antibiotic therapy. Figure adapted from Rupnik *et al*. (2009). Red line represents relative normal gut flora levels; green lines represents relative CDI risk.

C. difficile spores can withstand a number of harsh environmental factors such as low pH, UV radiation, high temperatures, and antibiotics (27, 31). Spores can survive on dry surfaces for up to 5 months (27, 31). The resilient nature of these spores allows them to contaminate highly-trafficked surfaces, making them easily transmissible. The spores are transmitted through the fecal-oral route, where diseased patients shed the spores in their stool, allowing the spores to

contaminate other surfaces (27). To minimize spore contamination, hospitals are advised to use 10% bleach solutions to disinfect surfaces and soap and water to disinfect hands (17, 31). Though 10% bleach is sufficient in eliminating *C. difficile* spores, it is crucial for hospitals to effectively train housekeeping staff in disinfecting practices. One study performed after a CDI outbreak showed that despite housekeeping staff using 10% bleach to disinfect rooms from discharged CDI patients, 24 out of 54 swabs of environmental surfaces tested positive for *C. difficile* growth after disinfection by the staff (32).

The spread of hypervirulent strains like PCR-ribotype 027, 078, as well as additional novel strains have also been deemed responsible for CDI incidences in health care facilities and within the community (33). Hypervirulent *C. difficile* strains have generally higher sporulation rates, increased toxin production, and are typically associated with outbreaks (27, 34). These characteristics are attributed to more severe CDI, increased chance of relapse, as well as higher mortality rates (27, 34).

Although hospital-acquired CDI is the most common form of transmission of the infection, community-acquired CDI has been on the rise (11). In fact, a 2012 population-based study in Minnesota reported that among the 385 cases of CDI, 41% of them were community-acquired (35). Alarmingly, community-acquired CDI is not usually associated with the same risk factors as hospital-acquired CDI (33). Community-acquired CDI incidences have been reported among children and young adults, as well as individuals who have not been exposed to antibiotics (33, 36).

1.1.4 *Antibiotic Resistance in* C. difficile

C. difficile is generally resistance to several antibiotic classes. In fact, Spigaglia (2016) reported that among 30 worldwide studies, 55% of clinical isolates were resistant to clindamycin, 51% were resistant to cephalosporins and 47% were resistant to fluoroquinolones (6). Of the clinical isolates resistant to cephalosporins (CFs), 79% were resistant to second-generation CFs and 38% were resistant to third-generation CFs (6). *C. difficile*'s antibiotic resistance is also in part responsible for the emergence of hypervirulent strains such as PCR ribotypes 027 and 078 (6). Approximately 30% of PCR ribotype 027 clinical isolates from North America were resistant to clindamycin, moxifloxacin, and rifampin (7). PCR ribotype 078 clinical and animal-derived isolates from humans and piglets with CDI have also been shown to be resistant to multiple antibiotics, like ciprofloxacin, erythromycin, imipenem, and moxifloxacin (7). Furthermore, the current antibiotics used to treat CDI are at risk of becoming ineffective towards *C. difficile*, as well.

Metronidazole, vancomycin, and fidaxomicin are the recommended antibiotics used to treat CDI. Alarmingly, clinical failures of CDI treatment using metronidazole or vancomycin have been reported (37, 38). These incidences could be explained by increased resistance to these drugs, though there is still no clear correlation of CDI reoccurrence with metronidazole or vancomycin resistance (37, 38).

A recent global meta-analysis of 60 studies reporting resistance rates of *C. difficile* isolates revealed an increase in vancomycin resistance and a slight decrease in metronidazole resistance (39). Before 2012, the weighted pooled resistance rate (WPR) was 0.4% for vancomycin and 2.5% for metronidazole (39). After 2012, the WPR rose to 4.0% for vancomycin but declined to 1.7% for metronidazole (39). The authors, however, suggested that

the decrease in metronidazole resistance might not translate as clinically significant and may in part be explained by the heterogeneity in susceptibility testing methods among the studies (39). Currently, there have been no reports of *C. difficile* resistance to fidaxomicin, the last line of defense against CDI (39). Given recent trends, it will not come to a surprise if fidaxomicin resistance reports emerge in the coming years.

1.2 ß-Lactam Antibiotics

1.2.1 *Brief History of ß-Lactam Antibiotics*

Ever since the serendipitous and revolutionary discovery of penicillin by Alexander Fleming in 1929 (40), ß-lactam antibiotics have been vital in combatting bacterial pathogens. Though Fleming's discovery of this groundbreaking substance occurred in the early 20th century, the first clinical trial on penicillin did not come into fruition until 1941 (41). The success of penicillin against streptococcal and staphylococcal infections in humans (41) intrigued pharmaceutical companies, enabling the mass production of penicillin and large-scale clinical trials (42). In 1945, Fleming and his colleagues were awarded the Nobel Prize in Physiology or Medicine for their discovery (42). Penicillin hit the market the following year (42).

Researchers began manipulating the R group surrounding the penicillin core (**Figure 1.3**). This led to the synthesis of penicillin derivatives (e.g. methicillin, ampicillin, and carbenicillin), expanding the range of antibiotic activity (42). Novel ß-lactam molecules were also isolated from other microbial species, like cephalosporins from *Cephalosporium acremonium* (42). Cephalosporins were the second sub-class of ß-lactams to be discovered (42, 43). Since the novel antibiotic was structurally distinct from penicillins, this further paved the way for scientists to synthesize an array of diverse broad-spectrum ß-lactams (42). Similarly,

scientists isolated the first monobactams and carbapenems, two other main sub-classes of ß-lactams, from microbes as well (42). Today, ß-lactams have become the most common antibiotic on the market. More than 65% of the total antibiotics worldwide comprise of ß-lactams (44).

1.2.2 *ß-Lactam Structure and Function*

1.2.2.1 *ß-Lactam Structure*

As their name suggests, ß-lactams are characterized by the presence of a ß-lactam ring within their molecular structure (**Figure 1.3**). Their structure mimics the D-alanyl-D-alanine peptidoglycan precursor, the natural substrate of penicillin-binding proteins (PBPs) (**Figure 1.3F**). Each sub-class of ß-lactams has a different core structure. Penicillins contain a 6-aminopenicillanic acid (6-APA) core, which is a natural fermentation product produced by *Penicillium chrysogenum* (**Figure 1.3A**) (45). Scientists realized that penicillins can be synthesized semi-synthetically by using 6-APA as a starting point, marking a pivotal moment for novel penicillin production (45). On the other hand, cephalosporins are synthesized by using 7-aminocephalosporanic acid (7-ACA) as the precursor which is not a natural fermentation product of *Cephalosporium acremonium* (**Figure 1.3B**) (45). Rather, scientists obtained 7-ACA by removing the R_1 side chain from naturally-occurring Cephalosporin C (45). To clarify, the R_2 group for 7-ACA is actually an ester derivative, but many cephalosporins are lacking this functional group, which is why it was omitted in the cephalosporin core structure in Figure 1.3B. Related to cephalosporins are the cephamycins, which are structurally identical to cephalosporins except for the presence of a methoxy group (**Figure 1.3C**). Finally, carbapenems are similar in structure to penicillins, cephalosporins, and cephamycins in that they are characterized by a fused ring to the ß-lactam core (**Figure 1.3E**). Unlike the rest of the ß-lactam family members,

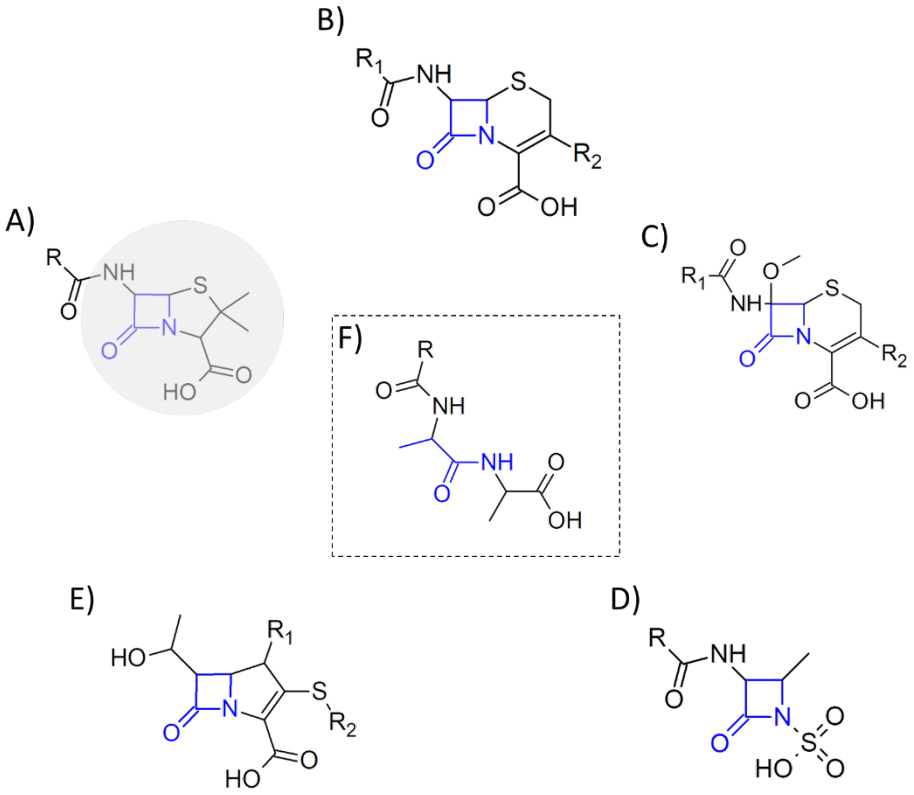

Figure 1.3. General structures of ß-lactam families in relation to PBP natural substrate. A) Penicillin core structure, 6-APA is highlighted in grey B) Cephalosporin core structure C) Cephamycin core structure D) Monobactam core structure E) Carbapenem core structure F) N-acyl-D-alanyl-D-alanine PBP natural substrate. For A-E, the ß-lactam ring is highlighted in blue. For F, the corresponding structural similarity to the ß-lactam ring is highlighted in blue.

monobactams lack the fused ring to the ß-lactam core and also contain a sulfonic acid group (46) (**Figure 1.3D**).

1.2.2.2 *ß-Lactam Function*

ß-lactams are bactericidal antibiotics that function by inducing a futile cycle of peptidoglycan synthesis and degradation, eventually causing cell lysis (47). The drugs mimic the natural substrate of penicillin binding proteins, enzymes responsible for peptidoglycan cross-linking and remodeling (48, 49).

Peptidoglycan is a mesh-like layer within the bacterial cell wall that is vital for cell wall

integrity and maintaining optimal osmotic pressure within the cell (50, 51). The layer is composed of polysaccharide chains of *N*-acetylglucosamine (NAG) and *N*-acetylmuramic acid (NAM) alternating subunits (52) (**Figure 1.4**). Each NAM subunit is linked to a pentapeptide.

The enzyme responsible for forming the glycosidic bond between the disaccharide pentapeptide Lipid II and the growing peptidoglycan chain is a transglycosylase (51, 53). D,D-transpeptidases cross-link the pentapeptide stems between the amino acid at the third position of the acceptor strand and the fourth amino acid of the donor strand, creating a 4→3 cross-link bridge. D,D-carboxypeptidases instead cleave the terminal D-alanine of the pentapeptide stem.

D,D-transpeptidases and D,D-carboxypeptidases share the same D-alanyl-D-alanine substrate. By definition, penicillin-binding proteins are enzymes that have D,D-transpeptidase or D,D-carboxypeptidase activity, but that can also sometimes harbor transglycosylase activity (52).

Bacteria can also use L,D-transpeptidases and L,D-carboxypeptidases to synthesize and remodel peptidoglycan (**Figure 1.4**). These enzymes differ from their penicillin-binding protein counterparts in that they recognize the two terminal amino acids in tetrapeptide stems. Tetrapeptide stems usually terminate in L-lysine-D-alanine or *meso*-diaminopimelate(*meso*-DAP)-D-alanine; the latter is found in *C. difficile* (54). The difference in terminal amino acids between pentapeptide and tetrapeptide stems means that L,D-transpeptidases and L,D-carboxypeptidases are not readily bound by ß-lactams.

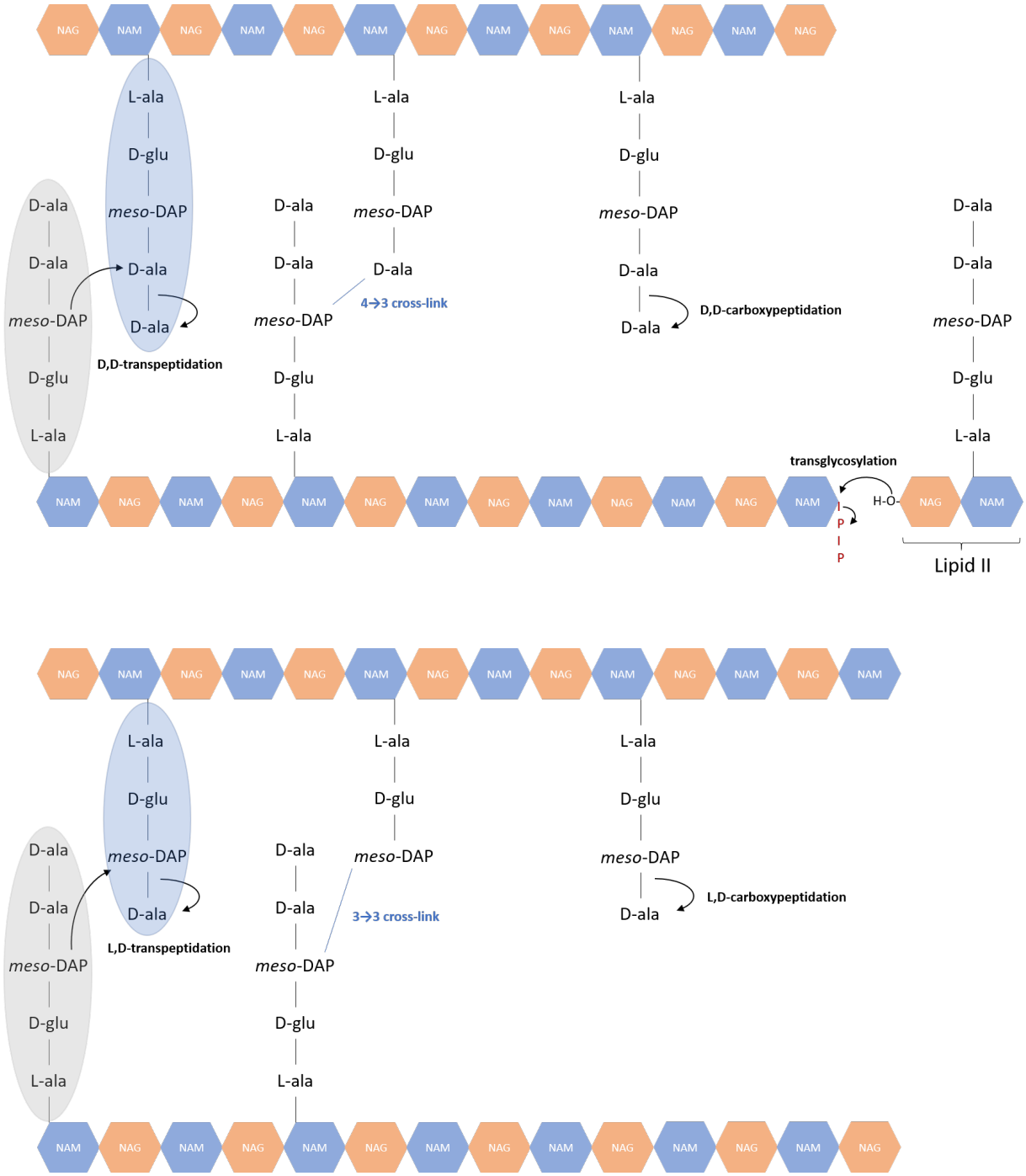

Figure 1.4. Select enzymatic reactions involved in peptidoglycan synthesis and remodeling. (Top) Enzymatic reactions shared among penicillin-binding proteins. (Bottom) Enzymatic reactions carried through by L,D-transpeptidases and L,D-carboxypeptidases. NAM: *N*-acetylmuramic acid NAG: *N*-acetylglucosamine. Donor peptide is highlighted in light blue. Acceptor peptide is highlighted in gray.

Transpeptidation and carboxypeptidation undergo similar two-step reactions (**Figure 1.5A**). In the first step, the carbonyl of the penultimate D-ala undergoes a nucleophilic attack by the catalytic PBP hydroxyl. Reformation of the carbonyl after the nucleophilic attack causes the cleavage of the terminal D-ala from the pentapeptide. The resulting structure is a reactive acyl-enzyme complex between the PBP and the now tetrapeptide. In the second step, either transpeptidation or carboxypeptidation will occur. For transpeptidation, the carbonyl of the acyl-enzyme complex undergoes a nucleophilic attack by the amine group from the third amino acid of the acceptor pentapeptide. Reformation of the carbonyl subsequently expels the PBP, resulting in the 4→3 cross-link bridge. For carboxypeptidation, the carbonyl of the acyl-enzyme complex undergoes a nucleophilic attack by a water molecule, which then leads to hydrolysis and disassociation of the PBP.

ß-lactams are similar in structure to the natural substrate of PBPs and can readily bind to the PBP active site (**Figure 1.5B**). Just like with the D-alanyl-D-alanine substrate, the PBP can form an acyl-enzyme complex with the ß-lactam ring. The complex formed between the PBP and the ß-lactam is, however, rather stable (50). The low rate of deacylation of the complex may be due to the steric hindrance of the nitrogen within the ß-lactam ring, thereby preventing a water molecule or an acceptor stem peptide from performing a nucleophilic attack on the carbonyl of the acyl-enzyme complex (50).

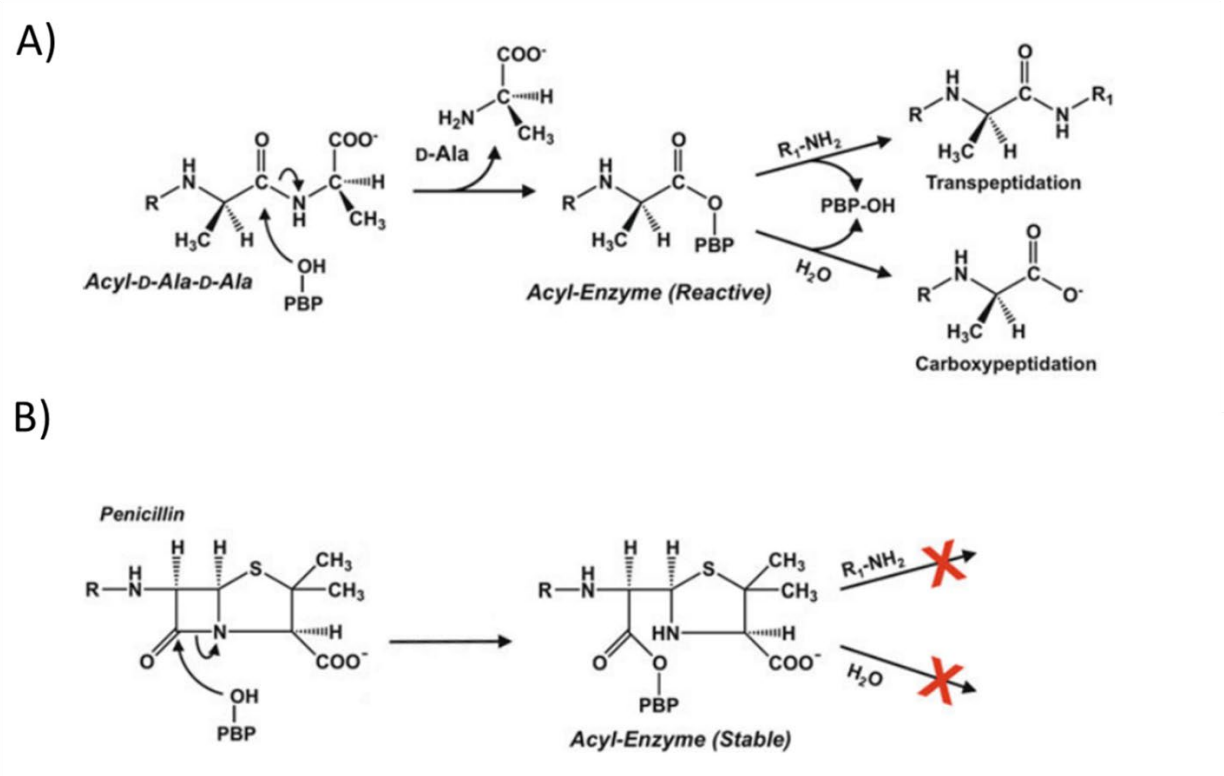

Figure 1.5. Reactions catalyzed by PBPs and ß-lactamases. Adapted from Nicholas & Davies (2012).

1.2.3 *Mechanisms of ß-Lactam Resistance*

Depending on the species, there are four mechanisms bacteria use in order to be resistant to ß-lactam antibiotics. Bacteria can produce ß-lactamases, harbor low-affinity PBPs, express efflux pumps, and modulate porin expression (44, 50, 55, 56). Decreasing membrane permeability through porin down-regulation, however, is specific for Gram-negative bacteria since Gram-positive bacteria lack the outer cell membrane in which porins exist.

A common mechanism of resistance against ß-lactams in Gram-positive bacteria is the expression of low-affinity PBPs. These PBPs can be acquired through mobile genetic elements, like transpeptidase PBP2a within *Staphylococcus aureus* (57). Conversely, originally susceptible PBPs can acquire resistance through mutations within or around the active site, as seen within

Staphylococcus pneumoniae and *Enterococcus faecium* (55). PBPs can either be upregulated in the presence of ß-lactams or more commonly can be constitutively expressed regardless of ß-lactam treatment (58). For example, in *S. aureus*, low-affinity PBP2a (*mecA*) lies within the *mec* operon and is de-repressed in the presence of ß-lactams (57). PBP2b and PBP2x in *S. pneumoniae*, however, are essential PBPs, and thus constitutively expressed, that have gained mutations in their sequences conferring low ß-lactam affinity (55, 58).

It has been suggested that the accumulation of mutations surrounding the active site and regions affecting the cleft opening select for the preferential binding of the natural PBP substrate rather than ß-lactams (55). As a compensatory mechanism, mutations within PBP2b were also found to solely improve transpeptidase activity instead of lowering ß-lactam affinity (59). Interestingly, it has also been reported that PBP2a in *S. aureus* harbors an allosteric binding domain that will bind natural PBP substrate (D-ala-D-ala terminus), as well as ß-lactam ceftaroline (60). Allosteric binding of either substrate triggers the opening of the active site through a conformational change, enabling the binding of either another stem pentapeptide or an additional ß-lactam (60). This discovery could give insight into an additional location in which mutations may arise (60).

Though less common, Gram-positive bacteria can also use ß-lactamases that are plasmid or chromosomally-encoded to inactivate ß-lactam antibiotics (**Figure 1.6**). These enzymes function similarly to PBPs in that they form an acyl-enzyme complex with the ß-lactam ring. This complex is quickly hydrolyzed, leaving the ß-lactam ring open and inactive. ß-lactamases can sometimes be induced and upregulated in the presence of ß-lactams (61–63).

Induced ß-lactamases are often regulated by a two-component regulatory system (TCS), like the *blaZ* operon within *S. aureus* regulating the ß-lactamase blaZ (57) or the ampC ß-

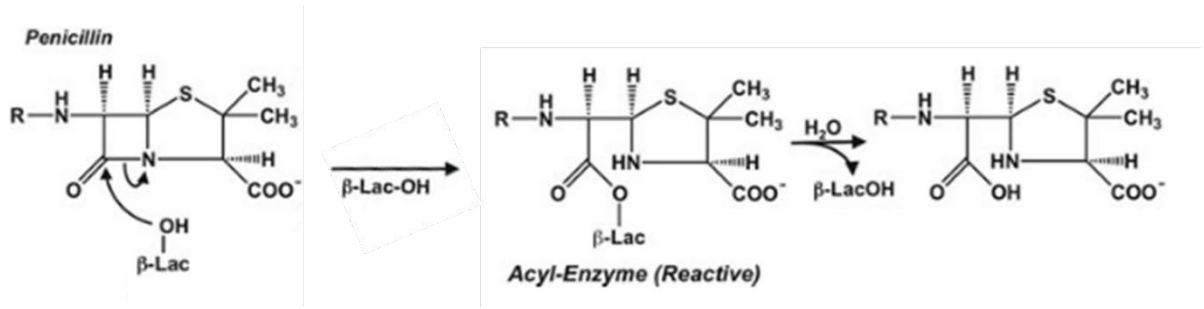

Figure 1.6. Reaction scheme for ß-lactamase mechanism. Adapted from Nicholas & Davies (2012).

lactamase in *Enterobacteriaceae* species (64). Other ß-lactamases, however, can be constitutively expressed regardless of ß-lactam expression, known as stable de-repression (65).

A non-specific mechanism for bacteria to evade antibiotics is through the use of efflux pumps. There are five families of efflux pumps in prokaryotes: the multidrug and toxic compound extrusion (MATE) family, the resistance-nodulation-division (RND) family, the small multidrug resistance (SMR) family, the major facilitator superfamily (MFS), and finally, the ATP-binding cassette (ABC) transporter superfamily (66). The RND family, however, is specific to Gram-negative organisms. Though the MFS family is the most studied in Gram-positive bacteria, ABC transporters have also been characterized as important drug exporters (66–70).

ABC transporters are the only family of efflux pumps that use ATP hydrolysis as the energy source (66). Virtually all ABC transporters contain two nucleotide binding domains (NBDs) and two transmembrane domains (TMDs) (71). The NBDs are responsible for ATP hydrolysis and the TMDs are responsible for creating the substrate translocation pathway across the cell membrane (71). In bacteria, ABC transporters exist as homodimers or heterodimers (71). Typically, one NBD is fused with one TMD in a single monomer, and then binds with another identical or structurally different monomer to form a homodimer or heterodimer, respectively

(71). Conversely, some prokaryotic heterodimeric ABC transporters are encoded by two open reading frames where one encodes a monomer with just the NBD, and the other encodes a monomer with only the TMD (67). The characterized multidrug ABC transporter of *Streptomyces peucetius*, DrrAB, in fact has this protein structure (67).

Multidrug ABC transporters are typically strictly regulated, and only activated in the presence of environmental effectors (66). Like ß-lactamases and PBPs described above, ABC transporters can be regulated by TCSs (72). These ABC transporters, though, are often associated with the export of antimicrobial peptides (71). The VraFG ABC transporter in *Staphylococcus aureus*, however, has been shown to be regulated by the GraRS two-component regulatory system and promote vancomycin resistance (73). Furthermore, ABC transporters can also be regulated by transcription factors. For example, the AbcA transporter in *S. aureus*, proven to expel ß-lactam antibiotics, is directly activated by the multiple antibiotic resistance regulator (MarR), MgrA, and repressed by the GntR-like transcriptional regulator, NorG (74). Some ABC transporters, however, can be constitutively expressed regardless of antibiotic exposure (68).

1.2.4 *ß-Lactam Resistance Mechanisms in* Clostridioides difficile

General mechanisms for antibiotic resistance in *C. difficile* range from acquiring mobile genetic elements (75), forming biofilms (76), to harboring resistance-associated genes within its chromosome (6, 77). The mechanisms conferring ß-lactam resistance in *C. difficile*, however, are largely unexplored.

Currently, genomic analysis of the *C. difficile* annotated genome is one of the only indicators for genes that might be involved in ß-lactam resistance. In 2016, Spigaglia published a list of 25 putative genes within *C. difficile* clinical strain 630 that might confer resistance to

cephalosporins, and presumably other ß-lactams (**Table 1.1**) (6). These genes encode putative ß-lactamases, ß-lactamase-like enzymes, PBPs, one signal-transducer and one transcriptional regulator. To elucidate the role of these genes in ß-lactam resistance, it would be worthwhile to measure expression changes for each gene before and after ß-lactam treatment.

Table 1.1. Locus-tags within *C. difficile* clinical strain 630 that might confer ß-lactam resistance. Taken from Spigaglia (2016).

Locus-tag in *C. difficile* 630	Product
CD630_03440	Putative β-lactamase-like protein
CD630_04580	Putative β-lactamase
CD630_04640	Putative β-lactamase-like hydrolase
CD630_04700	β-lactamase-inducing penicillin-binding protein
CD630_04710	Penicillinase transcriptional regulator
CD630_05150	D-alanyl-D-alanine carboxypeptidase, S11 peptidase family
CD630_05270	Putative β-lactamase-like hydrolase
CD630_05480	Putative penicillin-binding peptidase
CD630_06550	Putative β-lactamase-like protein
CD630_07810	Putative penicillin-binding protein
CD630_08290	Putative metallo-β-lactamase superfamily protein
CD630_08950	Metallo-β-lactamase superfamily exported protein
CD630_11480	Putative penicillin-binding protein
CD630_12290	Peptidoglycan glycosyltransferase
CD630_12910	Penicillin-binding protein
CD630_13740	Putative β-lactamase-inhibitor protein II
CD630_14690	Putative cell surface protein; putative penicillin-binding protein cwp20
CD630_16270	D-alanyl-D-alanine carboxypeptidase (penicillin-binding protein)
CD630_18020	Putative hydrolase, metallo-β-lactamase superfamily
CD630_21410	Serine-type D-Ala-D-Ala carboxypeptidase
CD630_24980	Putative sporulation-specific penicillin-binding protein
CD630_26560	Stage V sporulation protein D (sporulation-specific penicillin-binding protein)
CD630_27420	Putative hydrolase β-lactamase-like
CD630_31960	Putative penicillin-binding protein
CD630_36510	Putative metallo-β-lactamase-like hydrolase

1.3 Hypothesis and Specific Aims

In the present study, we aimed to elucidate any putative ß-lactamases and PBPs or additional resistance mechanisms that may be responsible in cephalosporin resistance. We

hypothesized that upon cephalosporin exposure, *C. difficile* would differentially express one or more of these putative resistance genes.

We first identified any additional putative ß-lactamases and transpeptidase or carboxypeptidase enzymes within the *C. difficile* 630 genome. Reverse-transcription quantitative PCR was then used to measure expression changes between untreated and cefoxitin-treated cells. Any genes that were considerably upregulated were deleted. Cephalosporin susceptibility of the null-mutants were measured against *C. difficile* 630 wildtype. Finally, RNA-sequencing was used to observe global changes in the transcriptome between untreated and cephalosporin-treated *C. difficile* strain 630.

1.4 Significance of Study

C. difficile is a serious nosocomial and community-acquired pathogen that can colonize and propagate in the gut of patients undergoing antibiotic therapy. Cephalosporins are still widely used today and have, in fact, been associated with *C. difficile* infection. In an effort to re-sensitize this pathogen to cephalosporins and other ß-lactams, it is important to unveil the mechanisms responsible for its resistance. None of the putative resistance genes listed above, nor the global transcriptome, have been studied with regard to ß-lactam resistance within *C. difficile* strain 630. Taking the first step in observing the transcription regulation changes during cephalosporin treatment is one of the first accounts in understanding ß-lactam resistance in *C. difficile*. The results from this study will help identify targets for the eventual development of novel therapeutic agents against *C. difficile*.

CHAPTER 2: Manuscript for the submission to the *Journal of Bacteriology*

Title: Differential gene expression analysis shows that ß-lactamases are not involved in cephalosporin resistance in *Clostridioides difficile* 630

Authors: Lara A. Turello[a], Amber Consul[a], Christopher Yip[a], Shirley Shen[b], Cale Seymour[a], Corey Geurink[b], Israel Alvarado[a], Ernesto Abel-Santos[a,b*]

Affiliations: [a] Department of Chemistry and Biochemistry, University of Nevada, Las Vegas, Las Vegas, Nevada, USA

[b] Nevada Institute of Personalized Medicine, University of Nevada, Las Vegas, Las Vegas, NV, 89154-4004

Contact: 4505 Maryland Parkway

Campus Box 4003

Las Vegas, NV 89154

Tel: (702) 895-2608

Fax: (702) 895-4072

Email: ernesto.abelsantos@unlv.edu

Keywords: *Clostridioides difficile*, *Clostridium difficile*, antibiotic resistance, antimicrobial resistance, ß-lactam resistance, ß-lactams, cephalosporins, ß-lactamase, penicillin-binding protein, RNA-Seq, transcriptome

2.1 Abstract

Clostridioides difficile infection (CDI) is the most common nosocomial infection worldwide. CDI has become a growing concern due to *C. difficile's* resistance to several antibiotics, including cephalosporins. Patients administered cephalosporins are at risk of contracting CDI. Cephalosporins are β-lactam antibiotics, which prevent bacterial cell wall synthesis by inhibiting penicillin-binding proteins (PBPs). β-lactam-resistant bacteria evade these antibiotics by producing β-lactamases or by harboring low-affinity PBPs. A genomic analysis of *C. difficile* strain 630 identified 31 putative ß-lactam resistance genes. These genes encode putative β-lactamase-like proteins and PBPs. We theorize that when *C. difficile* 630 is exposed to cephalosporins, a subset of these genes will be differentially expressed. Upon cefoxitin exposure, ß-lactamase blaCDD was upregulated approximately 600-fold. Deletion of the *blaCDD* locus led to little change in cephalosporin susceptibility. Expression analysis of the genes within the Δ*blaCDD* mutant under cefoxitin exposure showed minimal change in expression compared to 630 wildtype. Deletion of upregulated PBP, *vanY*, was also ineffective at increasing cephalosporin susceptibility. These data imply that there are additional mechanisms in which *C. difficile* 630 is resistant to cephalosporins. Global transcriptomic analysis of *C. difficile* 630 under the treatment of cephradine, cefoxitin, ceftazidime, and cefepime revealed the shared upregulated of a putative heterodimeric ABC transporter that is genomically located directly downstream of *blaCDD*. Further functional analysis will be necessary to elucidate this ABC transporter's role in cephalosporin resistance. Future studies will be geared towards using transposon mutagenesis to reveal cephalosporin resistance genes that are constitutively expressed regardless of ß-lactam treatment.

2.2 Introduction

Clostridioides (Clostridium) difficile infection (CDI) is the most common hospital-acquired infection in the United States (7). There are approximately 500,000 CDI incidences per year, and 29,000 of those incidences result in patient death within 30 days of diagnosis (21). CDI also poses an economic burden on the country, costing the government upwards of $5.4 billion dollars, annually (10).

Under stress*, C. difficile* forms resistant and dormant spores. Spores do not cause disease, but serve as infective vehicles for CDI. These structures can contaminate hospital surfaces for long periods (31), and can be eventually ingested by susceptible patients. Upon activation by bile salts and amino acids (28), spores are believed to germinate into toxin producing bacteria in the gastrointestinal (GI) tract of the host.

The natural gut microbiome in healthy individuals is capable of metabolizing *C. difficile* germinants, such as bile salts, thereby preventing spore germination in the GI tract (78). However, upon antibiotic treatment, the patients' natural gut microbial flora is depleted, leading to an accumulation of conjugated bile salts in the gut (78). This environment, in turn, allows for the germination of the spores into toxin-producing cells that colonize the GI tract, causing disease (78). Thus, the main risk factor associated with CDI is gut dysbiosis caused by aggressive antibiotic treatment (17, 24, 25).

C. difficile's pathogenicity is in part due to its intrinsic resistance to an array of antibiotics, including ß-lactams, fluoroquinolones, and macrolides (6, 7, 79). In fact, between 2012 and 2015, 55% of clinical isolates were resistant to clindamycin, 47% were resistant to fluoroquinolones, and 51% were resistant to cephalosporins (6). Of the 51% of isolates that were resistant to cephalosporins, 79% were resistant to second generation cephalosporins and 38%

were resistant to third generation cephalosporins (6). These percentages of resistance among clinical isolates could very well be exacerbated by the frequency in which ß-lactams are prescribed.

ß-lactams are one of the most commonly prescribed antibiotics with over 122 million outpatient prescriptions dispensed annually in the US (https://www.cdc.gov/antibiotic-use/community/programs-measurement/state-local-activities/outpatient-antibiotic-prescriptions-US-2017.html). Not only is *C. difficile* resistant to ß-lactams' mechanism of action, but this antibiotic family can trigger CDI (17, 24, 80). Moreover, patients who are prescribed second- or third-generation cephalosporins are believed to be at a greater risk of contracting CDI (24).

Cephalosporins are a part of the ß-lactam class of antibiotics. ß-lactam antibiotics restrict bacterial growth by inhibiting cell wall formation. ß-lactams mimic the D-alanyl-D-alanine dipeptide substrate of penicillin-binding proteins (PBPs) (48). Once bound, the ß-lactam forms an stable acyl-enzyme with the PBP and inhibits further peptidoglycan (PG) cross-linking (48). This triggers the bacterial PG biosynthesis machinery to undergo a useless round of PG synthesis and degradation, leading to cell death (47).

Gram-positive bacteria counteract ß-lactams by either expressing PBPs with low-affinity for the ß-lactam as well as using multidrug efflux pumps (e.g. ATP-binding cassette (ABC) transporters) to expel antimicrobials out of the cell (55, 58, 66). Less commonly Gram-positive bacteria also produce ß-lactamases which hydrolyze the ß-lactam ring within the antibiotic.

ß-lactamases are often triggered when bacteria are exposed to ß-lactams (61–63). These enzymes can be upregulated through a two-component system (TCS), like the ampC ß-lactamase in certain species within the *Enterobacteriaceae* family (64). Similarly, expression of PBPs can be triggered through this system, as seen with PBP2a in *Staphylococcus aureus* (57). PBPs , and

less commonly ß-lactamases, can also be constitutively expressed regardless of the presence of ß-lactams (58, 65). Likewise, ABC transporters expression can also be triggered by a TCS in the presence of environmental stressors like antibiotics (72, 73) or be constitutively expressed (68). Bacteria can also evade ß-lactamases by expressing enzymes known as L,D-transpeptidases and L,D-carboxypeptidases, collectively referred to as LDTs. These enzymes also function by cross-linking and remodeling peptidoglycan. However, they differ from PBPs in that they create 3→3 cross-links instead of 4→3 cross-links of the PG precursors.

Recently, Spigaglia compiled a list of putative resistance genes that could be potentially involved in ß-lactam (i.e. cephalosporin) resistance within the *C. difficile* clinical strain 630 (6). These loci, are thought to encode either ß-lactamases, ß-lactamase regulatory proteins, ß-lactamase-like proteins, or PBPs. However, functional analysis of these genes needs to be completed in order to confirm their involvement in ß-lactam resistance. Although *C. difficile* resistance to ß-lactam antibiotics is a prominent issue, characterization of the mechanisms involved in its resistance is lacking (6, 7).

In this work, we screened for differential expression under cephalosporin treatment of 31 putative ß-lactam resistance genes in *C. difficile* strain 630. As previously reported (81), we found that upon cefoxitin exposure, locus CD630_04580, (*blaCDD)* was overexpressed nearly 600-fold. Consistent with other reports (82), deletion of the *blaCDD* locus did not diminish *C. difficile* 630's resistance to cefoxitin. Transcriptional analysis of cefoxitin-treated *blaCDD*-null mutant, showed similar putative ß-lactamase and PBP expression patterns as the wild-type strain, suggesting that none of the tested genes compensate for the loss of *blaCDD*. Under cefoxitin treatment, locus CD630_16270 listed as a putative low-molecular weight PBP but functionally a D,D-dipeptidase (83), *vanY*, was the second-highest upregulated gene in both 630 wildtype and

blaCDD-null strains. However, deletion of *vanY* led to marginal decreases in resistance to four tested cephalosporins. These results emphasize the complexity of ß-lactam resistance in *C. difficile* and the need to elucidate the interplay between different resistance mechanisms involved.

In an effort to further identify mechanisms in which *C. difficile* might evade cephalosporins, we performed a global transcriptomic analysis of *C. difficile* strain 630 under the exposure of four cephalosporins. The most striking result was the significant upregulation of a putative heterodimeric ABC transporter encoded by loci CD630_04590 and CD630_04600. This result was conserved between all four cephalosporin treatments. These genes are immediately downstream of *blaCDD* but do not seem to be part of the same operon. We hypothesize that this putative efflux pump could be pumping the ß-lactams out of the cell, effectively evading cell wall synthesis inhibition. Future experiments will be geared towards deleting this putative ABC transporter within *C. difficile* strain 630 and observing any changes in cephalosporin susceptibility. Transposon mutagenesis will also be used against *C. difficile* strain 630 in order to identify important cephalosporin resistance genes that are constitutively expressed regardless of antibiotic treatment.

2.3 Materials and Methods

2.3.1 *Bacterial strains, reagents, and plasmids*

C. difficile strain 630 was obtained from the American Type Culture Collection (ATCC) and 630Δ*ermΔpyrE* was a generous gift from Prof. Aimee Shen from Tufts University in Boston, MA. Strains 630Δ*ermΔpyrEΔblaCDD*, 630Δ*ermΔpyrEΔblaCCDΔvanY*, and 630Δ*ermΔpyrEΔvanY* were generated for this study. *E. coli* strain Mach1 was purchased from Invitrogen (Waltham, MA), and HB101 was purchased from Promega (Wisconsin, MA). The *E. coli* strain HBCA434 was generated by transforming strain HB101 with conjugation plasmid pRK24.

Plasmid pCR-Blunt™ was purchased from Invitrogen as a part of the Zero Blunt™ PCR Cloning Kit. Plasmid pRK24 was purchased from Addgene (Watertown, MA). Plasmid pMTL-YN3 was generated By Prof. Nigel Minton at the University of Nottingham, UK and was a generous gift from Prof. Aimee Shen at Tufts University in Boston, MA.

Bacto™ Brain Heart Infusion broth and Difco™ agar (BD Biosciences) were purchased from VWR (Radnor, PA). Antibiotics and L-cysteine were purchased from Sigma-Aldrich (St. Louis, MO). EconoTaq® PLUS GREEN 2X Master Mix was purchased from Lucigen (Middleton, WI). Restriction enzymes, Phusion High-Fidelity DNA polymerase, RNA*later*®, the PureLink® RNA Mini Kit, and the TURBO DNA-*free*™ Kit were purchased from Invitrogen (Waltham, MA); qScript® cDNA SuperMix and PerfeCTa SYBR® Green SuperMix were purchased from QuantaBio (Beverly, MA). The SureSelect^{XT} RNA Direct Kit and SureSelect^{XT} Custom 1Kb-499kb library Kit were purchased from Agilent Technologies (Santa Clara, CA).

2.3.2 *Bacterial growth conditions*

C. difficile strains were grown in Bacto™ Brain Heart Infusion (BHI) broth supplemented with 5 g/L yeast and 1 g/L L-cysteine (BHIS). For antimicrobial susceptibility testing, BHIS was supplemented with liquid suspensions of either cephradine, cefoxitin, ceftazidime, or cefepime, as needed. BHIS agar plates were supplemented with 20 g/L yeast and 1 g/L L-cysteine. *C. difficile* strains were grown anaerobically at 37°C on a rocking platform at constant speed. *E. coli* strains were grown in Bacto Luria Bertani (LB) broth or solid media supplemented with liquid suspensions of kanamycin, thiamphenicol, and/or cefoxitin when appropriate. *E. coli* strains were grown aerobically at 37°C on an orbital shaker at constant speed.

2.3.3 *Identification of Putative ß-lactam Resistance Genes*

The NCBI "Gene" database was used by using search terms "ß-lactamase" and "penicillin-binding protein" against the *Clostridioides difficile* strain 630 annotated genome (Genome assembly: ASM920v2). Any additional loci not listed by Spigaglia (6) were considered as putative ß-lactam resistance genes. Sequences greater than 400 amino acids were considered to likely be high molecular-weight PBPs (84). Sequences shorter than 400 amino acids were considered to likely be low molecular-weight PBPs, L,D-transpeptidases/carboxypeptidases, or ß-lactamases (84).

2.3.4 *Antibiotic Susceptibility Testing*

Streak-plate lawns of mutant and wild-type *C. difficile* strains were swabbed and inoculated into 5 mL of BHIS broth, respectively. The overnight cultures were then sub-cultured by individually diluting 1:1000 into a series of BHIS broth aliquots supplemented with 2-fold

increasing concentrations of antibiotic. Cultures were then placed onto a constant speed rocker and incubated anaerobically at 37°C. Minimum inhibitory concentrations (MIC) were determined after 48 hours of incubation by observing the minimum concentration of antibiotic in which bacterial turbidity was not visible. The highest concentration of antibiotic that allowed cell growth was labeled as the half-MIC. Bacteria growing at the half-MIC were used for qPCR analysis.

2.3.5 *RNA Isolation and Purification*

A 5 ml suspension of *C. difficile* strain 630 or 630Δ*erm*Δ*pyrE*Δ*blaCDD* treated with 0 or 128 (half-MIC) µg/mL cefoxitin-, were collected at mid to late exponential phase and diluted to an OD_{600} of 0.4 in 3 mL (~10^9 bacterial cells) of BHIS broth. Cells were centrifuged for 5 minutes at 1583 rcf. Supernatants were decanted and cell pellets were resuspended in 750 uL RNA*later*® (Invitrogen) and stored at room temperature for up to one week or at 4°C for up to one month.

RNA*later*® was removed by centrifuging the samples for 5 minutes at 1583 rcf and decanting the supernatant. Total RNA was extracted using PureLink® RNA Mini Kit (Invitrogen) following manufacturer's instructions, except for the cell-lysing step. To facilitate lyses, 100 mg of glass beads were added to each bacterial suspension and vortexed for 5 minutes. Extracted total RNA was resuspended in 50 µL nuclease-free water and stored at -80°C. Successful RNA extraction was confirmed using the NanoDrop 1000 Spectrophotometer.

Before conversion to cDNA, total RNA extracts were treated with the TURBO DNA-*free*™ Kit (Invitrogen) following either the routine or rigorous DNase treatment protocol. DNA-free total RNA extracts were further purified using ethanol precipitation as follows: 0.1 vol 3M

sodium acetate and 2.5 vol of 100% ethanol were added to the samples and the resulting samples were stored overnight at -20°C. Ethanol was removed by centrifugation at 21130 rcf at 4°C for 10 minutes. The resulting RNA pellets were washed with 2.5 vol 70% ethanol, followed by 2.5 vol 100% ethanol. RNA pellets were centrifuged at 21130 rcf at 4°C for 5 minutes between ethanol washes. The RNA pellets were air-dried and resuspended in 50 µL of nuclease-free water. The purity of DNA-free total RNA extracts was determined using the NanoDrop 1000 Spectrophotometer. RNA extracts were considered acceptable if the A260/A280 ratio was greater than 1.8 and the A260/A230 ratio was 1.5 or greater. RNA samples that were used for RNA-Seq analysis were concentrated to a concentration of approximately 100 ng/uL using the CentriVap (Labconco) prior to cDNA library preparation, if needed.

Prior to cDNA synthesis, the presence of residual genomic DNA contamination within the pure RNA extracts was assessed. A final concentration of 5 ng/µL of RNA was subjected to PCR, alongside a positive control containing genomic DNA and a negative control where the template was replaced with water. The primers used were those targeting the reference gene *rpsJ* (85). The absence of the appropriate size band for the PCR reactions containing RNA as template confirmed the successful removal of genomic DNA. RNA integrity was measured using the Agilent Bioanalyzer. All RNA samples had RNA integrity scores greater than 7.0.

2.3.6 *cDNA Synthesis and qPCR Assays*

The purified RNA obtained above was reverse-transcribed using the qScript® cDNA SuperMix kit (QuantaBio) following manufacturer's instructions. qPCR primer sets targeting putative ß-lactam resistance genes within *C. difficile* 630 were designed using the PrimerQuest Tool provided by Integrated DNA Technologies, Inc (**Table S1**). The primer set for reference

gene, *RpsJ*, was has been already published (85), and was chosen because of its minimal regulation variability between antibiotic treatments.

The PerfeCTa SYBR® Green SuperMix (QuantaBio) system was used to determine relative gene expression levels following the relative standard curve method (86). On each qPCR plate, a five-point standard curve of serially diluted wild-type *C. difficile* strain 630 genomic DNA was used to quantify RNA transcript levels while adjusting for reaction efficiency (**Equation A1**). Primers were used at a final concentration of 5 μM, and cDNA was added at a final concentration of 1 ng/uL for genes on interest, and 0.1 ng/uL for the reference gene. Quality control was determined by including no template controls (NTCs) for all primer sets on each plate, and no reverse transcription (NRT) controls for each new batch of reverse-transcribed RNA. Any amplification within the NRT controls that occurred at a corrected Cq greater than 5 cycles later than its corresponding cDNA sample was considered negligible. All control and experimental groups were run in technical triplicates on each plate (**Figure A1**) using the following thermal cycling conditions: 95°C for 5 min; 40 cycles of 95°C for 5 min, 61°C for 30s, 72°C for 30s; followed by a melting curve ranging from 50°C to 95°C in 5s increments. The relative normalized expression (RNE) ratio (**Equation A2**) and regulation (**Equation A3**) were calculated using the Bio-Rad CFX Manager™ Software version 3.1 using default settings. As the software default, the threshold for differential expression was set as a 4-fold change in regulation. The software automatically performed a paired-end student's t-test on the differential expression, setting the significance threshold at $P < 0.01$.

2.3.7 *Construction of plasmid to generate* C. difficile *strain 630ΔblaCDD strain*

An 856 bp region upstream and a 907 bp downstream of *blaCDD* were PCR amplified using Phusion High-Fidelity DNA polymerase (Invitrogen) and independently cloned into a pCR-Blunt vector. The vectors were transformed into donor *E. coli* Mach1 cells. Transformed *E. coli* cells were selected on LB agar supplemented with 50 μg/mL kanamycin.

Upon pCR™-Blunt::insert extraction, inserts and plasmid pMTL-YN3 (87) were digested with appropriate restriction enzymes (upstream region: [5'] BamHI and [3'] XbaI; downstream region: [5'] XbaI and [3'] NotI) and ligated together to generate the *blaCDD* knockout construct, pMTL-YNΔblaCDD. The identity of pMTL-YNΔblaCDD was confirmed by Sanger sequencing (GeneWiz). The pMTL-YNΔblaCDD vector was transformed into the conjugative *E. coli* strain CA434 for mating with *C. difficile* 630Δ*ermΔpyrE*. Transformed E. coli CA434 were plated on LB agar supplemented with 25 μg/mL chloramphenicol and 100 μg/mL ampicillin and incubated at 37°C. Glycerol stocks were prepared and stored at -80ºC until needed.

2.3.8 *Construction of plasmid to generate* C. difficile *strain 630ΔvanY strain and ΔblaCDDΔvanY strain*

To generate the *VanY*-null mutant, we followed the Gibson assembly procedure (88). Briefly, the "16270 upstream homology FWD" and "16270 SOE REV" primer set was used to PCR amplify the upstream homologous region. Likewise, the "16270 downstream homology REV" and "16270 SOE FWD" primer set was used to PCR amplify the downstream homologous region. Phusion High-Fidelity DNA polymerase (Invitrogen) was used for these amplification steps. The PCR products were then purified and fused using splicing by overlap extension (SOE). Plasmid pMTL-YN3 was linearized by digestion with AscI and SbfI restriction enzymes.

The fused construct and the digested pMTL-YN3 were then combined and incubated with T5 exonuclease, Phusion High-Fidelity DNA polymerase, and T4 DNA ligase and incubated at 50ºC for 1 hour.

2.3.9 *Allelic Exchange and Selection*

To obtain *C. difficile* mutants, we followed the procedure developed by Kuan *et al.* (87). *E. coli* CA434 harboring each mutagenic plasmid was grown in 5 mL LB broth containing 25 µg/mL chloramphenicol and 100 µg/mL ampicillin for approximately 6 hours. Simultaneously, *C. difficile* 630Δ*ermΔpyrE* or 630Δ*ermΔpyrEΔblaCDD* were grown anaerobically for 6 hours in 5 mL BHI broth. The 5 mL *E. coli* culture was centrifuged at 1583 rcf for 5-10 minutes and the supernatant was decanted. The resulting pellet brought into the anaerobic chamber and was gently resuspended with 1 mL of the *C. difficile* 630Δ*ermΔpyrE* culture. The bacterial resuspensions were mated by plating seven 100 ul drops into BHIS plates. Bacteria were allowed to conjugate for up to 16 hours under anaerobic conditions. The bacterial mixtures were transferred onto BHIS plates containing 10 µg/mL thiamphenicol, 15 µg/mL kanamycin, and 8 µg/mL cefoxitin ($BHIS_{TKC}$) and incubated for 3 days to select for successful conjugation and plasmid uptake by *C. difficile*. 6 to 9 individual *C. difficile* colonies were re-streaked onto BHIS plates supplemented with 15 µg/mL thiamphenicol, 15 µg/mL kanamycin, and 8 µg/mL cefoxitin ($BHIS_{T15KC}$) to drive chromosome integration of the knockout construct. 6 to 9 individual colonies were serially passaged four to six times onto $BHIS_{T15CK.}$ After $BHIS_{T15CK}$ selection, 6 to 8 colonies were re-streaked onto *C. difficile* minimal media (CDMM) (89) supplemented with uracil and 5-fluoro-ororate (5-FOA) to negatively select for single-site integrants and positively-select for double recombinants. To identify true double recombinants, *C. difficile* colonies that

successfully grew on CDMM plates were used for colony PCR using flanking primers (**Table S1**). *BlaCDD*-null mutant recombinants yielded a PCR fragment of 1993 bp, while wild-type recombinants yielded a 2866 bp PCR fragment (**Figure S1**).

2.3.10 *Confirmation of mutant identity during MIC analysis*

Aliquots of the half-MIC cultures were diluted 8-fold in nuclease-free water and used as PCR template using primers that flank *blaCDD* and *vanY* (**Figure S1**). The PCR served as a quality control check to confirm that there was no cross-contamination of strains during cephalosporin treatment. The thermal cycling conditions were: 98ºC for 2 min; 40 cycles of 98ºC for 10 sec, 53ºC for 20 sec, and 72ºC for 1 min. and 45 sec; followed by a final extension step at 72ºC for 5 min. and infinite hold at 4ºC. The PCR products were then run against a 1 kb ladder on a 1% agarose gel at 130 constant volts.

2.3.11 *Sample treatment and collection for RNA-Seq analysis*

C. difficile 630 wild-type was streaked onto three BHIS plates. The three plates were considered to be biological triplicates. A swab from each plate was inoculated into three 5 mL BHI broths supplemented with 5 g/L yeast and incubated overnight. The overnight cultures were sub-cultured into 14 mL BHI broth supplemented with either cephradine, cefoxitin, ceftazidime, or cefepime. 630 wild-type was treated with 256 µg/mL cephradine, 128 µg/mL cefoxitin, 128 µg/mL ceftazidime, and 32 µg/mL cefepime. Cultures were grown to exponential phase and diluted using fresh BHI broth to an OD_{600} of 0.4 in a total volume of 3 mL. Note: in lieu of some samples having been collected more towards late-log/early stationary phase, we decided to recollect those samples at mid-log phase. The samples that were recollected were all labeled as

"X-2", where X is the treatment. The diluted cultures were centrifuged at 1583 rcf for 5 minutes and the supernatants were decanted. The cell pellets were resuspended in 750 µL of RNALater® and kept at 4ºC until further processing. To ensure that the cultures were collected during exponential phase, a minimum of one additional OD_{600} reading was taken of the uncollected portions of each culture in the subsequent hours post-sample collection. If the OD_{600} increased during subsequent hours, it was evident the culture was collected during exponential phase. Glycerol stocks were made of each culture and stores at -80ºC. RNA isolation and purification protocols are the same as those described above.

2.3.12 *Preparation of cDNA libraries*

The kits used for library preparations were the SureSelect^{XT} HS and XT low input enzymatic fragmentation Kit (Agilent Technologies), SureSelect^{XT} RNA Direct Kit (Agilent Technologies), the RNA custom design XT2 baits for *C. difficile* 630 (Agilent Technologies), and a SureSelect XT HS target enrichment system for Illumina Paired-end multiplexed sequencing library Kit (Agilent Technologies). Briefly, 100 ng of total RNA input were fragmented into 150 bp fragments using the RNA Fragmentation Mix. The RNA fragments were then reverse-transcribed into double-stranded cDNA using the RNA-Seq First Strand Master Mix followed by the Agilent Second Strand and End Repair Enzyme Mix. Sample-specific Barcode adaptors were then ligated to the 3'- and 5'-ends of the fragments. The adaptor-ligated fragments were enriched through 8-14 PCR cycles. The amplified library was purified and selected for 300 bp fragments using Beckman Coulter AMPure XP beads. The quality of the pre-captured library was assessed using the Agilent Bioanalyzer. The library was then slowly hybridized for 20 hours to *C. difficile* 630-specific baits created by Agilent Technologies. The hybridized library was

then captured using streptavidin beads and amplified through 8-13 PCR cycles. The amplified cDNA library purified using AMPure XP beads and checked again using the Agilent Bioanalyzer. The purified cDNA library was sequenced using the Illumina Nextseq 500 sequencer.

2.3.13 *RNA-Seq data analysis*

Reads were mapped against the annotated *C. difficile* 630 genome (Genome assembly: ASM920v2). Quality control and initial analysis was performed using CLC Genomics Workbench 12.0 (https://www.qiagenbioinformatics.com/). Briefly, raw reads were trimmed using a modified-Mott trimming algorithm (90) and a quality limit of 0.05 was used. Adapters were trimmed, along with read regions containing more than 2 ambiguous bases. Analysis was performed using the RNA-Seq analysis tool. The Identify and Annotate Differentially Expressed Genes and Pathways workflow on CLC Genomics Workbench 12.0 was used to identify differentially expressed genes and pathways. The workflow was customized for prokaryotes.

Samples were first visualized using a principal component analysis (PCA) plot to compare the transcriptomic profiles between biological replicates and between treatment groups using R v3.6.3 with the ggplot2 package and *prcomp* function and using log-TPM for normalized read counts. Ellipses around sample clusters were generated using the *stat_ellipse* function and represent 95% confidence. Genes that were differentially expressed were determined using a false discovery rate (FDR) cut-off of $P < 0.05$ and a fold-change >2.0. The Kyoto Encyclopedia of Genes and Genomes (KEGG) Pathways Database was used for analysis of differentially regulated KEGG orthology (KO) identifiers assigned to specific pathways (https://www.genome.jp/kegg/tool/map_pathway.html). A Venn-diagram of shared statistically

significantly upregulated genes (FDR $P < 0.05$ and > 2-fold change) was created using the online tool Venny (https://bioinfogp.cnb.csic.es/tools/venny/).

2.3.14 *Linear regression analysis of RT-qPCR expression data versus RNA-Seq expression data*

The RT-qPCR data were transformed to a log2 scale by taking the $\log_2$ of the absolute value of the fold-change. The same was done for the RNA-Seq data. Finally, the two log2-transformed data series were plotted against each other in a scatter plot. A linear regression analysis was performed in GraphPad Prism v8.4.0, and a correlation coefficient (R^2) was obtained.

2.4 Results

2.4.1 *The genome of* C. difficile *strain 630 contains 31 putative ß-lactam resistance genes*

A recent publication identified 25 putative ß-lactam resistance genes (6). In order to identify any additional putative ß-lactam resistance genes within *C. difficile* strain 630, we searched the NCBI "Gene" database using search terms "ß-lactamase" and "penicillin-binding protein" against *Clostridioides difficile* 630 genome. We found six additional putative ß-lactam resistance genes, bolded in Table 1 and Table S1. The loci were annotated as: a putative muramoyltetrapeptidase (CD630_13390), a hypothetical protein containing a D,D-carboxypeptidase domain (CD630_14060), a D,D-carboxypeptidase with a "vanY-like" structure (CD630_25040), two hypothetical proteins harboring transpeptidase domains (CD630_29630 and CD630_30070), and finally another D,D-carboxypeptidase (CD630_36010). Based on these annotations, we added these six loci to the original list of 25 putative ß-lactam resistance genes for RT-qPCR analysis.

2.4.2 *Optimization of RNA purification*

Purified and un-degraded RNA is essential for qPCR and RNA-Seq analyses. Following crude RNA extraction, we measured the purity of the samples by using the Nanodrop Spectrophotometer (**Table A1**). Some of the RNA-Seq samples measured at an A260/A230 below 1.5. However, upon DNase-treatment and ethanol precipitation, these values rose well above 1.5, an acceptable purity level for RNA-Seq analyses (**Table A2**).

The DNA-free purified RNA extracts were then tested for any residual gDNA contamination by running PCR reactions using purified RNA samples as template and comparing with *C. difficile* 630 gDNA template (**Figures A2, A3, A4, and A5)**. For the RNA-Seq samples

"ctrl 1-2" and "A 1", bands appeared when RNA was used as template for the PCR reaction (**Figure A3 (A)**). However, upon two more rounds of DNase-treatment, any residual gDNA was eliminated (**Figure A3 (B)**). For qPCR wildtype RNA sample "cfx #1", a faint band appeared when using the RNA as template for the PCR reaction (**Figure A4 (A)**). Though this sample was not re-treated with DNase, the RNA was used as template for a no reverse-transcription control (NRT) against cDNA that was reversed transcribed from the same RNA sample and loaded at equal concentrations. The amplification curve in the NRT control showed that the residual gDNA falls within negligible levels for qPCR analyses (**Figure A4 (B)**). The *blaCDD*-null mutant RNA extracts were all free of residual gDNA, as well (**Figure A5**).

Finally, the integrity of the DNA-free RNA extracts was measured using the Agilent Bioanalyzer (**Table A3**). Nearly all of the RNA samples yielded an RNA Integrity Number (RIN) greater than 9.5. The lowest RIN was 7.9, which belonged to qPCR RNA sample "wildtype ctrl RNA #2". A few of the sample technical replicates did not yield a RIN, but at least one of the replicates within each group, did. Manual analysis of the electrophoretograms for Bioanalyzer technical replicates with no RIN confirmed that the RNA samples were, indeed, suited for qPCR and RNA-Seq analyses.

2.4.3 *Optimization of qPCR assays*

To control for the specificity of the primers used to quantify transcription of the putative ß-lactam resistance genes, we performed PCR using *C. difficile* strain 630 genomic DNA as template against each primer set and running the PCR products on an agarose gel. All qPCR primer sets yielded the correct amplicon size listed in Table S1. The qPCR primer sets were then tested for their efficiency using a *C. difficile* strain 630 genomic DNA standard curve (**Figure**

A6). Figure A6 only includes a standard curve for the *rpsJ* primer set, but serves as an example of the standard curves obtained with all 31 primer sets. Most of the efficiencies of the primers ranged between 80.1-89.7%, but five primer pairs ranged between 70.5-80.1% efficiencies. (**Table A4**). The R^2 values for 22 of the standard curves ranged between 0.996-0.999. The remaining R^2 values ranged between 0.990-0.996, and only one yielded an R^2 value of 0.987. Finally, the specificity of each primer set was checked again by analyzing the melting curve after qPCR amplification (**Figure A7**). Each primer set yielded a single peak, re-confirming the specificity of the primer sets. All melting temperatures were greater than 72.0 ºC (**Table S1**).

2.4.4 *Of the genes tested from* C. difficile *strain 630, class D ß-lactamase blaCDD and D,D-dipeptidase vanY are the most upregulated under cephalosporin pressure*

Wild-type *C. difficile* strain 630 shows a MIC of 256 µg/mL for cefoxitin. To determine upregulation of potential ß-lactam resistance genes, we treated a liquid inoculum of *C. difficile* strain 630 with a sub-inhibitory concentration of cefoxitin (128 µg/mL) in parallel to an untreated culture. Most of the 31 putative ß-lactam resistance loci within cefoxitin-treated wild-type *C. difficile* strain 630 were upregulated from 1.1- to 3.2-fold and did not exceed the threshold for true differential expression according to CFX Manager default settings (**Figure 1; Table 3; Table S3**). Putative ß-lactamases CD630_03440, CD630_06550, and CD630_04640 were upregulated 1.7-, 2.1-, and 2.0-fold, respectively, whereas CD630_36510 was downregulated 1.7-fold.

Among the putative penicillin-binding proteins, CD630_07810 and CD630_11480 were upregulated 2.1 and 3.2-fold. Loci with unclear protein domains CD630_14060, CD630_25040, CD630_31960, and CD630_36010 were slightly differentially expressed, as well.

CD630_14060, CD630_25040, and CD630_36010 were upregulated 2.1-, 2.7, and 2.4-fold, respectively, whereas CD630_31960 was downregulated 1.3-fold. Transcriptional regulator, CD630_04710, was upregulated 3.0-fold, as well as a putative BlaR1-like signal transducing protein, CD630_05480, by 1.5-fold. Finally, a putative BLIP II protein, CD630_13740, was upregulated 1.3-fold. The remaining sixteen loci did not have statistically significant changes in expression.

Only two loci, CD630_04580 and CD630_16270, were upregulated above the threshold of 4-fold expression change (**Table S3**). The most striking upregulation observed was for locus CD630_04580 that encodes a recently characterized class D ß-lactamase (*blaCDD)* (82). *BlaCDD* gene transcription was induced 577.1-fold upon cefoxitin-treatment. In contrast, the second-most upregulated locus, CD630_16270 encoding D,D-dipeptidase *vanY*, was induced 9.6-fold. The P-values for the changes in expression of *blaCDD* and *vanY* were $5x10^{-6}$ and $3.8x10^{-5}$, respectively.

2.4.5 *blaCDD and vanY confer marginal resistance to ß-lactams*

Through allelic exchange, we created a *C. difficile blaCDD*-null mutant. Interestingly, even though *blaCDD* is strongly upregulated during cephalosporin treatment, the *C. difficile blaCDD*-null mutant showed only a 2-fold decrease in cefepime and ceftazidime resistance (**Table 2**).

We also created a single knockout mutant missing *vanY* and a double-knockout mutant missing both *blaCDD* and *vanY*. The *vanY*-null mutant showed a 2-fold decrease in cefepime resistance. Similar to the *blaCDD*-null mutant, the double-knockout mutant showed a 2-fold decrease in both ceftazidime and cefepime.

2.4.6 C. difficile *blaCDD-null mutant and wild-type have similar putative ß-lactam resistance gene expression profiles*

To test whether the *C. difficile blaCDD*-null mutant compensated for the gene deletion by upregulating one or more of the remaining putative resistance loci, we performed transcriptional analysis for the *C. difficile blaCDD*-null mutant under cefoxitin treatment (**Figure 1**). Interestingly, regulation of the remaining loci was not drastically different compared to wild-type *C. difficile* strain 630. The loci that seemed to be slightly more upregulated in the *blaCDD*-null mutant were CD630_04700 (*blaR*), CD630_04710 (*blaI*), CD630_06550, CD630_16270 (*vanY*), and CD630_36010 which all surpassed the 4-fold threshold of upregulation. Signal transducing protein *blaR* and transcriptional repressor *blaI* increased their expression by approximately 1.7- and 2.3-times more in the *blaCDD*-null mutant compared to wild-type, respectively (**Figure 1; Table S3**). Putative ß-lactamase-like protein, CD630_06550, and putative D,D-carboxypeptidase, CD630_36010, were approximately 2- and 3-times more expressed in the *blaCDD*-null mutant, respectively. Finally, *vanY* was 1.6-times more upregulated in the *blaCDD*-null mutant compared to wildtype, where the RNE ratio yielded for wild-type was 9.6 and 15.6 for the mutant.

2.4.7 *Cephradine, ceftazidime, and cefepime, but not cefoxitin -treated* C. difficile *show similar transcription profiles as untreated cells*

We separately treated *C. difficile* strain 630 cells with sub-inhibitory concentrations of cephradine, ceftazidime, and cefepime. The resulting RNA samples were analyzed for changes in the transcriptome compared to untreated cells. Principal component analysis (PCA) showed that

samples treated with cephradine (A), ceftazidime (C), and cefepime (D) clustered with the untreated samples (Ctrl) (**Figure 3**). A 95% confidence ellipse surrounding the untreated samples, indeed, encompasses the cephradine-, cefazidime-, and cefepime-treated samples, as well. One replicate of the ceftazidime-treated group, WtC1, plotted outside of the ellipse around the untreated samples. In contrast, cefoxitin treated cells formed a distinct cluster separated from all other samples. Only one cefoxitin treated sample, WtB1, clustered with both ellipses.

We then analyzed the number of KEGG orthology (KO) identifiers that are assigned to KEGG pathways, and that were differentially expressed after cephalosporin treatment (**Table S4**). We specifically examined KEGG pathways that are involved in metabolism and environmental signalling. We saw that cefoxitin-treated cells upregulated a higher number of KO identifiers related to amino acid and secondary metabolite biosynthesis pathways. Cefoxitin-treated cells also upregulated a higher number of KO identifiers relating to ABC transporters and phosphotransferase systems.

2.4.8 *Transcription profiles between qPCR analyses and RNA-Seq analyses are comparable*

We analyzed the reproducibility of the RT-qPCR and RNA-Seq data from *C. difficile* strain 630 treated with cefoxitin to the (**Table 3; Figure 2**). The fold-change differences between the RT-qPCR data and RNA-Seq data are rather similar. The fold-change in *vanY* expression was 9.64 upon RT-qPCR analysis, and 6.64 upon RNA-Seq analysis. The greatest change in expression calculated between the two methods was for *blaCDD*. For RT-qPCR, we observed an upregulation of 577.07 upon cefoxitin treatment, but for RNA-Seq the upregulation was merely measured at 21.03-fold. Nevertheless, *blaCDD* remained as the most upregulated locus among the 31 putative ß-lactam resistance genes after RNA-Seq analysis. A linear regression analysis

plotting the log2-transformed fold-change for qPCR data against the log2 transformed fold-change for RNA-Seq data resulted in a correlation coefficient $R^2 = 0.8094$ (**Figure 2**).

2.4.9 *BlaCDD and a downstream putative heterodimeric ABC-transporter are upregulated across cephalosporin treatments*

We further compared the transcription profile of all cephalosporin-treated samples to identify which shared genes were statistically significantly upregulated among the four cephalosporin treatments (**Figure 4**). The shared upregulated genes included a hypothetical membrane protein (CD630_04570), *blaCDD* (CD630_04580), a putative ATP-binding cassette (ABC) transporter ATP-binding protein (CD630_04590), a putative ABC transporter permease (CD630_04600), and a putative amino acid ABC transporter permease (CD630_21750).

The hypothetical membrane protein (CD630_04570) has been shown to be part of the same operon as *blaCDD* and are thus co-transcribed (81). In our RNA-Seq, analysis CD630_04570 was the most upregulated locus under every cephalosporin treatment, ranging from approximately 54- to 391-fold upregulation. The second-most upregulated gene for each cephalosporin treatment was *blaCDD* (CD630_04580), which ranged from 11- to 52-fold. It is peculiar, however, that the hypothetical membrane protein appears to have a considerably higher fold-change with respect to the ß-lactamase, given that they are suggested to be co-transcribed (81).

The putative ABC transporter ATP-binding protein (CD630_04590) and the putative ABC transporter permease (CD630_04600) are both upregulated at approximately equal levels in each cephalosporin treatment: an 8-fold increase for cephradine, 9.5-fold increase for cefoxitin, 17-fold increase for ceftazidime, and 5-fold increase for cefepime. The putative amino acid ABC

transporter permease (CD630_21750) is the least upregulated of the five shared genes ranging from 2.3- to 4.6-fold for each cephalosporin treatment.

2.5 Discussion

Despite the clinical relevance of CDI, the intrinsic resistance *C. difficile* to ß-lactam antibiotics has been poorly characterized (6, 82). Consistent with previous work (81, 82), gene expression analysis of 31 putative ß-lactam resistance genes in wildtype *C. difficile* strain 630 revealed that class D ß-lactamase, *blaCDD*, was drastically upregulated in the presence of a sub-inhibitory concentration of cefoxitin (**Figure 1**). Indeed, we see small changes in regulation among most of the other tested genes.

A similar transcription profile was recently reported when *C. difficile* strain 630Δ*erm* was treated with different ß-lactams (81). Sandhu *et al*. observed that *blaCDD* was upregulated between 800- and 1100-fold upon cefoperazone, ampicillin, or imipenem treatment (81). They measured the transcriptional changes in several other putative ß-lactamases, as we did, but saw minimal changes in regulation after treatment with any of the three ß-lactams. They also measured the transcriptional changes for three other putative ß-lactamases that we did not test in our RT-qPCR analyses: CD630_06920, CD630_24780, and CD_19300. The authors saw minimal changes in these loci, as well. We replicated these observations in our RNA-Seq analyses, however.

We initially believed that *blaCDD* would be greatly involved in cephalosporin resistance, due to its higher upregulation compared to the remaining loci. Surprisingly, deletion of *blaCDD* led to no change in resistance against cephradine or cefoxitin and just a 2-fold decrease in the MIC for ceftazidime and cefepime. The observed change in MICs are comparable to previously published data (82). Our MICs, however, are overall 2- to 4- fold higher than those reported by Toth *et al.* (82). This could be explained by the difference in antimicrobial susceptibility testing

methods. Nevertheless, these minimal phenotypic changes suggest that one or more alternative resistance genes are compensating for the *blaCDD* gene deletion.

Comparing gene expression analysis between wild-type *C. difficile* strain 630 and a *C. difficile blaCDD*-null strain revealed little change in expression of the remaining putative resistance genes upon cefoxitin treatment. There was no obvious compensation of ß-lactamase or PBP expression in the *blaCDD*-null mutant. Hence, ß-lactam resistance seems to be multifactorial, likely involving low-affinity PBPs, efflux pumps, and/or other ß-lactam-evading mechanisms. As far as ß-lactamases, previous studies (81, 82) already demonstrate that *blaCDD* is likely the only functional ß-lactamase in *C. difficile* strain 630Δ*erm*, and that there are no ß-lactamases being constitutively expressed. These results further steer attention to other possible resistance mechanisms.

ß-lactam resistance could be in part due to low-affinity PBPs, as seen in methicillin-resistant *Staphylococcus aureus* (MRSA) and other Gram-positive and Gram-negative bacteria (91–93). These PBPs can acquire mutations within and around their active site that favor their natural substrate rather than the ß-lactam (55, 59). Like ß-lactamases, PBPs can be a controlled by two-component regulatory systems that are activated by ß-lactams and in turn upregulate the low-affinity enzyme (58). Conversely, PBPs can be constitutively expressed, regardless of ß-lactam exposure (58). Identifying the PBPs within *C. difficile* strain 630 could provide valuable insight in other enzymes responsible for ß-lactam resistance.

Through our gene expression analyses, we were able to determine if any of these PBPs were upregulated in the presence of cefoxitin. The only putative PBP that seemed to be moderately upregulated was CD630_16270 (*vanY*) (**Figure 1**). We noticed that expression of *vanY*, previously explored in its possible contribution to vancomycin-resistance (83, 94),

increased from approximately 10-fold in wildtype *C. difficile* strain 630 to 16-fold in the *C. difficile blaCDD*-null strain. We, thus, explored *vanY*'s contribution to cephalosporin resistance as we did with *blaCDD*.

Glycopeptides like vancomycin function by inhibiting cell wall synthesis, but unlike ß-lactams, they bind to the terminal D-ala-D-ala of pentapeptides and inhibit PBPs (95). Bacteria can evade glycopeptides by harboring a set of *van* genes involved in cleaving the terminal D-ala from the pentapeptide stem and replacing the amino acid with D-ser or D-lac (95). *VanY* resides in a cluster of genes referred to as the *vanG*-like cluster. These functionally characterized genes comprise a two-component regulatory system involving a *vanR* that encodes a response regulator and a *vanS* that encodes a signal-transducing histidine kinase (83). This two-component system regulates the downstream *vanG* gene that encodes a D-ala : D-ser ligase, the *vanY* gene that encodes a D-ala-D-ala dipeptidase, and a *vanTG* gene that encodes an L-ser and L-ala racemase (83). However, it has been previously shown that despite the upregulation of these genes in the presence of a sub-inhibitory concentration of vancomycin, *C. difficile* is still susceptible to the antibiotic (83, 94). Though no D,D-carboxypeptidase activity was observed for *vanY* (83), we hypothesized that *C. difficile* 630 might be upregulating *vanY* as a low-affinity PBP to counteract cephalosporins.

Like with *blaCDD*, we generated a *C. difficile* strain 630 mutant with a complete deletion of *vanY*, as well as a mutant with complete deletions of both *vanY* and *blaCDD*. We observed that the only phenotypic change for the *vanY*-null mutant was a 2-fold decrease in cefepime resistance. The double-knockout mutant showed a 2-fold decrease in both ceftazidime and cefepime. *VanY* has been previously shown to only have D,D-dipeptidase activity (83). This enzyme activity is similar to *vanX*, a gene involved in vancomycin resistance that cleaves D-ala-

D-ala dipeptides in order for D-ala-D-ser dipeptides to be ligated to tripeptide precursors, instead (96). Since we only observed a 2-fold MIC decrease for cefepime for the *vanY*-null mutant, it is unclear whether *vanY* was functioning as a modified PBP, or if the gene deletion was being compensated by other putative low-affinity D,D-carboxypeptidases and D,D-transpeptidases.

Although bacteria can express both low-affinity essential and nonessential PBPs to counteract ß-lactams (93, 97, 98), they can mostly evade these antibiotics by using L,D-transpeptidases and L,D-carboxypeptidases to synthesize peptidoglycan. These enzymes are collectively referred to as LDTs. ß-lactams have little to no activity against these enzymes, as their substrate is L-lys-D-alanine or *meso*-Diamonipimelate(*meso*-DAP)-D-alanine. A recent study investigated the ability of copper chloride ($CuCl_2$) to inhibit LDTs in *Escherichia coli* and *Enterococcus faecium* (99). The study found that subminimum inhibitory concentrations of $CuCl_2$ decreased the MIC for ampicillin 16- and 128-fold for *E. coli* and *E. faecium*, respectively (99). These results indicated that inhibition of LDTs abolished the bacterium's ability to bypass ß-lactams (99).

Among the 30 loci we studied, two harbor L,D-transpeptidase/carboxypeptidase domains: CD630_29630 and CD630_30070. It has been shown that *C. difficile* strain 630Δ*erm* has L,D-transpeptidase activity encoded by loci CD630_29630 and CD630_27130, referred to as Ldt_{Cd1} and Ldt_{Cd2} (54). The study also found that ampicillin- exposure increased L,D-transpeptidase-specific 3→3 crosslinks in peptidoglycan precursors, and decreased the D,D-transpeptidase-specific 4→3 crosslinks (54). *C. difficile* 630Δ*erm*'s susceptibility to ampicillin despite the increased activity of the L,D-transpeptidases suggested that D,D-transpeptidases are essential for cell viability (54). However, approximately 75% of *C. difficile* strain 630's peptidoglycan is crosslinked by these L,D-enzymes (54), suggesting that they too are major contributors to cell

viability. It was later shown that Ldt_{Cd1} has L,D-carboxypeptidase activity, whereas Ldt_{Cd2} and Ldt_{Cd3} (CD630_30070) have both L,D-transpeptidase and L,D-carboxypeptidase activity *in vitro* (100). Interestingly, Ldt_{Cd1} and Ldt_{Cd2} were capable of being acylated and sufficiently inactivated by carbapenems, but still were able to evade other ß-lactams like cephalosporins and penicillins (100). It would be worthwhile to further elucidate the role of LDTs in ß-lactam susceptibility in *C. difficile* when all three of its LDTs discussed above are deleted. It could be that deleting all three LDTs will abolish *C. difficile*'s ability to evade certain ß-lactams.

As previously described, 31 coding sequences within *C. difficile* 630 were identified as putative ß-lactam resistance genes. A literature review reveals a discrepancy in distinguishing which loci to classify as putative ß-lactamases or PBPs (6, 18, 77, 81). This could in part be due to the idea that ß-lactamases evolved from penicillin-binding proteins, making it challenging to distinguish between the two enzyme clades (101). In order to evade the ambiguity of certain coding sequences, as well as include untested putative ß-lactam resistance coding sequences, we expanded expression analyses to a global level through RNA-Seq. Our goal was to also reveal any additional antibiotic resistance mechanisms.

We observed that cells treated with cephradine, ceftazidime, and cefepime clustered together with untreated bacteria. This observation suggests that cephalosporin treatment has little impact on the global transcription of *C. difficile* vegetative bacteria. In contrast, cefoxitin-treated cells cluster independently from all other samples. This phenotype could be partially explained by the length of time that the cefoxitin-treated cells were incubated. For the untreated, cephradine-, ceftazidime-, and cefepime-treated groups, the cells were collected no later than 24 hours after treatment. The cefoxitin-treated cells were incubated for approximately 35 hours before collection because of the slow growth rate of the cells at 128 µg/mL of cefoxitin. The

prolonged incubation period may have triggered the transcription of starvation-specific pathways not seen in the transcription profiles of the other treated groups. In fact, we see a higher number of upregulated KEGG orthology (KO) identifiers associated with amino acid and secondary metabolite biosynthetic pathways, as well as phosphotransferase systems, in the cefoxitin-treated group compared to the other groups (**Table S4**).

Members of the inorganic phosphate (Pi) regulatory system, *pstC*, *phoU*, and *pstB*, were also substantially upregulated in the cefoxitin-treated group. The Pi regulatory system, also known as the Pho regulon is responsible for upregulating its genes upon limited external Pi (102). Proteins encoded by *pstC* and *pstB* are a part of the pstSCAB phosphate ABC transporter, whereas *phoU* encodes an auxiliary protein involved in phosphate uptake regulation (102). Genes involved in thiamine biosynthesis, *thiG*, *thiH_1*, and *thiE2* were also considerably upregulated. The upregulation of these genes have been previously related to nutrient starvation (103, 104). It must be noted, however, that the 2-dimensional PCA plot only accounted for 51% of the total variance seen among the samples, meaning that some of the variance between samples may have been lost. Further in-depth data analysis of these global transcriptomic responses after cephalosporin exposure will be necessary.

In any case, between all four treated groups, we saw the shared upregulation of five loci, four of them clustering together: CD630_04570 through CD630_04600 (**Figure 2.4B**). The operon formed by CD630_04570 and CD630_04580 encodes a hypothetical membrane protein and adjacent ß-lactamase, *blaCDD*, respectively. This observation, along with previously published data (81, 82), suggests that this operon is activated upon exposure to a range of ß-lactam antibiotics. The two downstream genes, CD630_04590 and CD630_04600, encode a putative heterodimeric efflux pump consisting of an ABC transporter ATP-binding protein and

an ABC transporter permease, respectively. However, a previous study found that upon exposing *C. difficile* strain 630 to a subinhibitory concentration of amoxicillin and performing a microarray analysis, only *blaCDD* was upregulated 11.70-fold among these four clustering genes (105). This could be attributed to the overall higher sensitivity of RNA-Seq technology compared to microarrays.

Efflux pumps are used by both eukaryotic and prokaryotic cells for a wide range of functions (66). A class of efflux pumps commonly used across all cells are ATP-binding cassette (ABC) transporters. The use of ATP-binding cassette (ABC) exporters, a subclass of ABC transporters, in prokaryotes are sometimes used to evade antibiotics (106). Prokaryotic ABC transporters are expressed as a homodimer or a heterodimer. For homodimers, the transmembrane domains (TMDs) and nucleotide-binding domains (NBDs) are fused within the same monomer, and then associate with another identical protein (70). For heterodimers, the TMDs and NBDs can be found within the same monomer, or are found within two separate and adjacent protein-encoding genes, creating a separate permease (TMD) and ATP-binding protein (NBD), respectively (70). Furthermore, ABC transporters can be triggered and upregulated by two component systems that lie adjacent either upstream or downstream of the efflux enzyme (72, 73). Examples of characterized multidrug ABC transporter heterodimers are the EfrCD transporter in *Enterococcus faecalis* (70) and the AnrAB transporter in *Listeria monocytogenes* (69), the latter of which was shown to effectively expel various ß-lactam antibiotics.

As previously mentioned, we observed the intriguing and statistically significant upregulation of coding sequences encoding a putative ABC transporter ATP-binding protein (CD630_04590), and an adjacent putative ABC transporter permease (CD630_04600) approximately 300 bp downstream of *blaCDD*. The two loci overlap each other, suggesting that

they are transcribed together and encode a heterodimeric ABC transporter. Moreover, a putative two component system lies directly downstream of the ABC transporter in the reverse orientation (**Figure 5**), possibly suggesting its role in activating the ABC transporter under environmental stress. The potential TCS comprises of a putative response regulator transcription factor table(CD630_04620) and a putative HAMP domain-containing histidine kinase (CD630_04610). Until now, only one ABC transporter has been functionally characterized within *C. difficile* strain 630, encoded by coding sequence CD630_20680 (107). The study found that this ABC transporter was upregulated from approximately 3- to 5-fold upon ß-lactam exposure, and successfully transported ethidium bromide when expressed in *E. coli* (107). Our RNA-Seq data, however, does not show significant differential expression of the CD630_20680 ABC transporter. Further functional analysis of these putative ABC transporters and their potential involvement in ß-lactam resistance will be necessary.

Other recent advancements have been made in elucidating ß-lactam resistance in *C. difficile*. In a recent paper, deletion of the transpeptidase domain of a cortex-specific PBP, *spoVD*, in *C. difficile* R20291 decreased the MIC for cefoxitin and ceftazidime by 4-fold (Y.A. Alabdali, P. Oatley, J.A. Kirk, and R.P. Fagan, submitted for publication). Though not stated in the article, it could be that the crosslinking activity of *spoVD* is essential for ß-lactam evasion and peptidoglycan synthesis upon cephalosporin exposure because the enzyme has a low-affinity for cephalosporins. This PBP is homologous to CD630_26560 in *C. difficile* strain 630 sharing over 99% identity. Neither our qPCR nor our RNA-Seq data show upregulation of this locus, suggesting that it is perhaps a constitutively expressed PBP.

The deletion of penicillin-binding and STK-associated serine/threonine kinase (PASTA-STK) *prkC* in *C. difficile* 630Δ*erm* also resulted in an increase in cephalosporin susceptibility

(108). The MICs for cefoxitin, ceftazidime, cefepime, and cefotaxime decreased by >6-, 20-, 17.5-, and 8-fold, respectively, upon *prkC* deletion (108). *PrkC* is responsible for the regulation of numerous downstream processes, such as cell wall metabolism, antibiotic resistance, and virulence (108). Interestingly, the *prkC*-null mutant did not show a change in PG composition compared to *C. difficile* 630Δ*erm* (108). The authors only observed an overall decrease in the amount of PG between *C. difficile* 630Δ*erm* and the *prkC*-null mutant. The authors suggested that this phenotype might be simply due to shorter glycan chains within the PG. The role of *prkC* in cephalosporin resistance remains unclear. Overall, these findings highlight the need to further clarify of the role of cell wall metabolism and regulation in ß-lactam resistance in *C. difficile*.

2.6 Tables and Figures

Table 2.1

Table 2.1. List of putative ß-lactam resistance genes within *C. difficile* 630

Number	Locus tag	Gene product
1	CD630_03440	Putative β-lactamase-like protein
2	CD630_04580 (blaCDD)	Putative β-lactamase
3	CD630_04640	Putative β-lactamase-like hydrolase
4	CD630_04700 (blaR)	β-lactamase-inducing penicillin-binding protein/ beta-lactamase class D
5	CD630_04710 (blaI)	Penicillinase transcriptional regulator
6	CD630_05150	D-alanyl-D-alanine carboxypeptidase, S11 peptidase family
7	CD630_05270	Putative β-lactamase-like hydrolase
8	CD630_05480	Putative penicillin-binding peptidase BlaR1-like protein
9	CD630_06550	Putative β-lactamase-like protein
10	CD630_07810	Putative penicillin-binding protein
11	CD630_08290	Putative metallo-β-lactamase superfamily protein
12	CD630_08950	Metallo-β-lactamase superfamily exported protein
13	CD630_11480	Putative penicillin-binding protein
14	CD630_12290	Peptidoglycan glycosyltranferase
15	CD630_12910 (dacF)	D-alanyl-D-alanine carboxypeptidase
16	CD630_13740	Putative β-lactamase-inhibitor protein II
17	**CD630_13990**	**Muramoyltetrapeptide carboxypeptidase**

18	**CD630_14060**	**Hypothetical protein (contains D-alanyl-D-alanine carboxypeptidase domain)**
19	CD630_14690	Putative cell surface protein, putative penicillin-binding protein cwp20
20	CD630_16270 (vanY)	D-alanyl-D-alanine carboxypeptidase (D,D-dipeptidase)
21	CD630_18020	Putative hydrolase, metallo-β-lactamase superfamily
22	CD630_21410	Serine-type D-ala-D-ala carboxypeptidase
23	CD630_24980	Putative sporulation-specific penicillin-binding protein
24	**CD630_25040**	**D-alanyl-D-alanine carboxypeptidase vanY-like**
25	CD630_26560	Stage V sporulation protein D [sporulation-specific penicillin-binding protein]
26	CD630_27420	Putative hydrolase β-lactamase-like
27	**CD630_29630 (LdtCd1)**	**Hypothetical protein (contains L-lys-D-alanine transpeptidase domain)**
28	**CD630_30070 (LdtCd3)**	**Hypothetical protein (contains L-lys-D-alanine transpeptidase domain)**
29	CD630_31960	Putative penicillin-binding protein/beta-lactamase class C
30	**CD630_36010**	**D-alanyl-D-alanine carboxypeptidase**
31	CD630_36510	Putative metallo-β-lactamase-like hydrolase

Bolded locus tags are genes that were added to the Spigaglia list of putative ß-lactam resistance genes after an NCBI “Gene” database search.

Figure 2.1

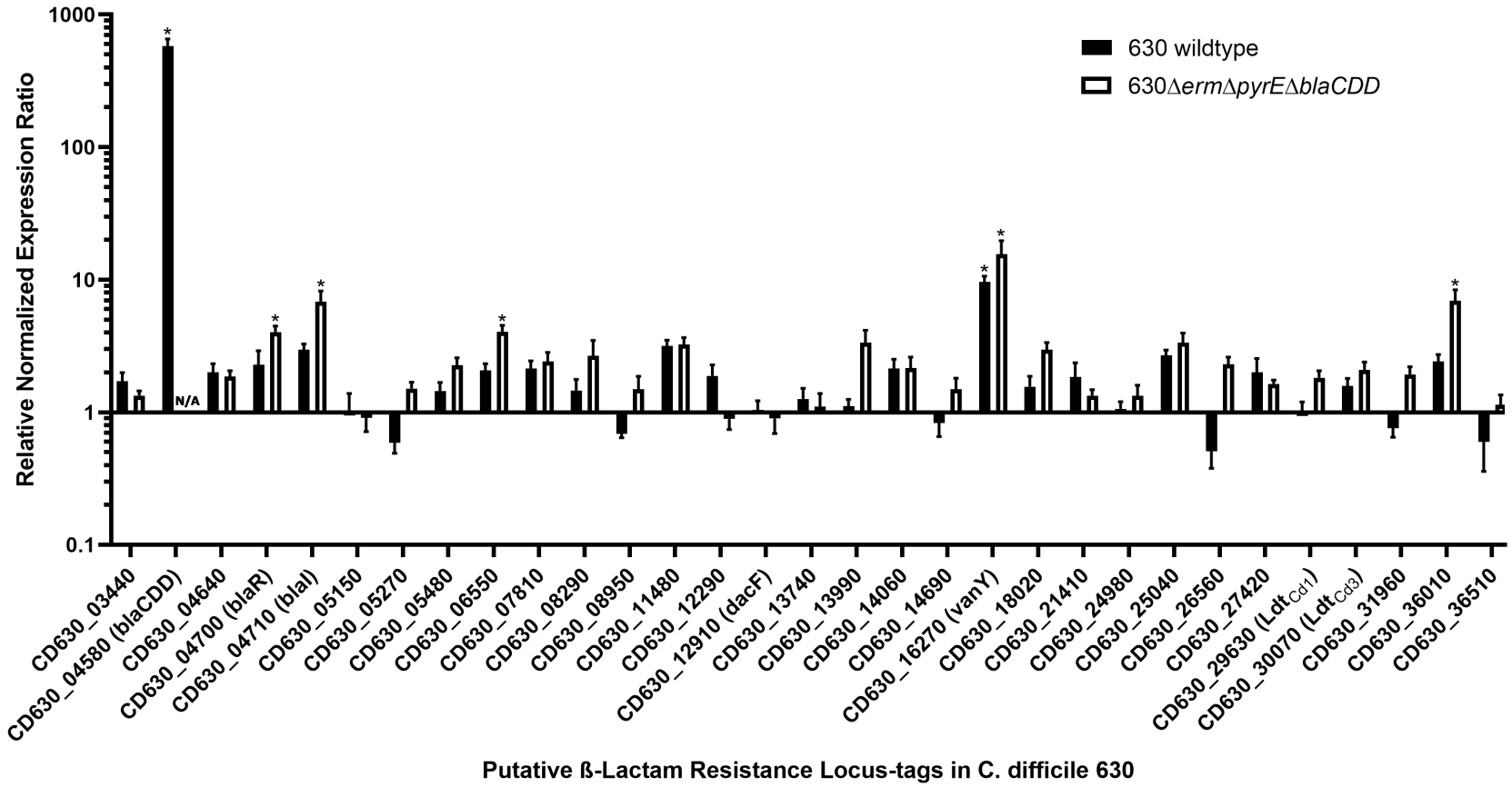

Figure 2.1 Relative normalized expression of putative ß-lactam resistance genes within *C. difficile* 630 and 630Δ*ermΔpyrEΔblaCDD* under cefoxitin treatment. Columns indicate the change in relative expression of the cefoxitin-treated sample in relation to an untreated sample. Relative expression change is normalized to housekeeping gene *rpsJ*. Error bars indicate the standard deviation of three technical triplicates. Asterisks indicate expression changes greater than 4-fold.

Table 2.2

Table 2.2. Cephalosporin susceptibility of *C. difficile* strains

Strain	Cephradine	Cefoxitin	Ceftazidime	Cefepime
630 wildtype	>256	256	256	256
630Δ*ermΔpyrEΔblaCDD*	>256	256	128	128
630Δ*ermΔpyrEΔvanY*	>256	256	256	128
630Δ*ermΔpyrEΔblaCDDΔvanY*	>256	256	128	128

Values reflect minimum inhibitory concentrations (MIC) in μg/ml. For cephradine, cefoxitin and ceftazidime, the average MIC of at least three independent experiments is listed. For cefepime, the median MIC of at least four independent experiments is listed.

Table 2.3

Table 2.3. Relative fold-change of *C. difficile* strain 630 under cefoxitin treatment

Locus tag	qPCR Fold-Change	RNA-Seq Fold-Change
CD630_03440	1.7	1.4
CD630_04580 (blaCDD)	577.1	21.0
CD630_04640	2.0	1.0
CD630_04700 (blaR)	2.3	2.7
CD630_04710 (blaI)	3.0	3.1
CD630_05150	1.0	-1.4
CD630_05270	-1.7	-1.5
CD630_05480	1.5	1.2
CD630_06550	2.1	1.3
CD630_07810	2.1	2.4
CD630_08290	1.5	1.0
CD630_08950	-1.5	-1.7
CD630_11480	3.2	2.0
CD630_12290	1.9	1.2
CD630_12910 (dacF)	1.0	1.2
CD630_13740	1.3	-1.2
CD630_13990	1.1	-1.4
CD630_14060	2.1	1.2
CD630_14690	-1.2	-1.8
CD630_16270 (vanY)	9.6	6.6
CD630_18020	1.6	-1.2
CD630_21410	1.8	1.1
CD630_24980	1.1	1.2
CD630_25040	2.7	-1.2
CD630_26560	-2.0	-1.3
CD630_27420	2.0	1.4
CD630_29630 (Ldt_{Cd1})	1.0	-1.5
CD630_30070 (Ldt_{Cd3})	1.6	-1.2
CD630_31960	-1.3	-1.5
CD630_36010	2.4	1.9
CD630_36510	-1.6	-2.5

Relative fold-changes listed are those calculated by BioRad CFX Manager and CLC Genomics Workbench for qPCR and RNA-Seq, respectively. Loci listed are only those tested using RT-qPCR.

Figure 2.2

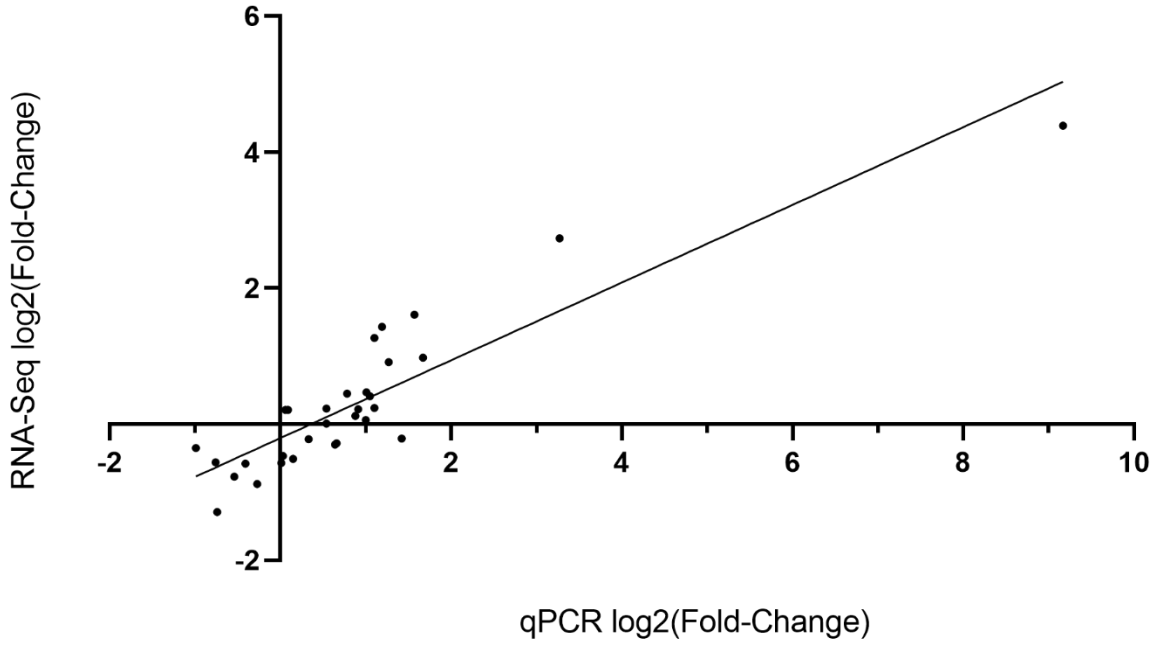

Figure 2.2. Correlation of RNA-Seq data with RT-qPCR data. RNA-Seq and RT-qPCR fold-change values were log2-transformed and plotted in a scatter plot. The R^2 of the best-fit line is 0.8094.

Figure 2.3

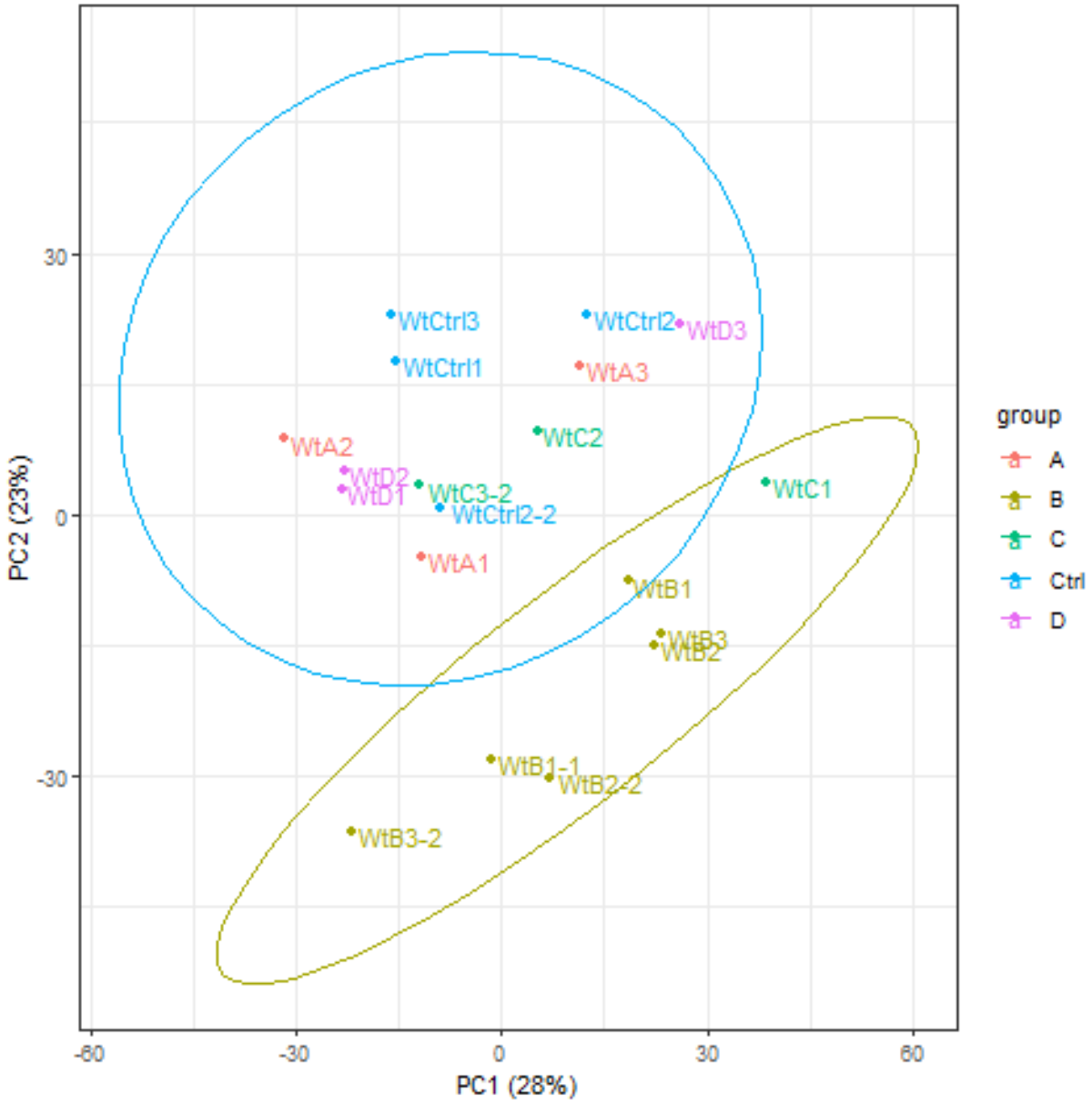

Figure 2.3. PCA plot depicting the clustering of cephalosporin-treated and untreated *C. difficile* strain 630 cells. A: cephradine treatment; B: cefoxitin treatment; C: ceftazidime treatment; D: cefepime treatment; Ctrl: control (untreated). In yellow, a 95% confidence ellipse was drawn around the cefoxitin-treated cells. In blue, a 95% confidence ellipse was drawn around the untreated cells.

Figure 2.4

A

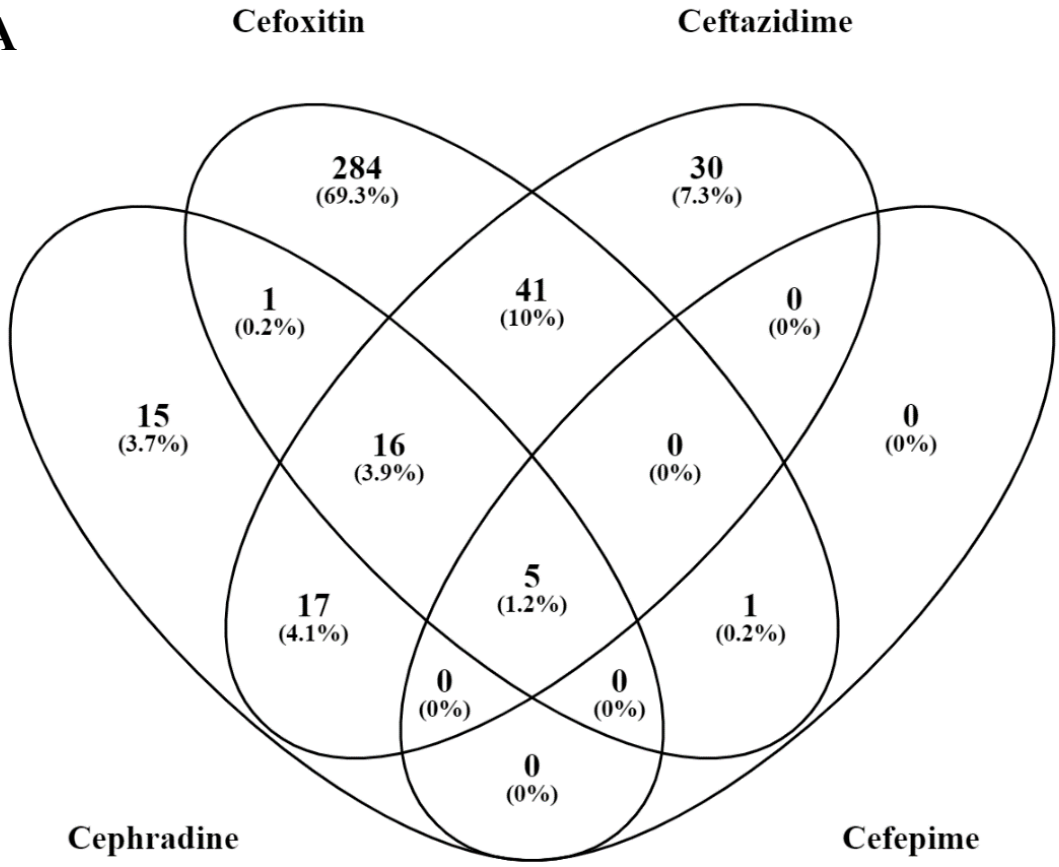

B

RNA seq statistically significant loci upregulated in all four cephalosporin treatments					
		Fold-Change			
Locus-tag	**Annotation**	**Cephradine**	**Cefoxitin**	**Ceftazidime**	**Cefepime**
CD630_04570	membrane protein	157.0	65.6	390.8	53.5
CD630_04580	ß-lactamase	17.8	21.0	52.2	11.2
CD630_04590	ABC transporter ATP-binding protein	8.6	9.9	19.8	5.3
CD630_04600	ABC transporter permease	7.3	9.2	16.4	4.4
CD630_21750	amino acid ABC transporter permease	2.9	2.7	4.6	2.3

Figure 2.4. Shared upregulated genes among cephalosporin treatments. (A) Venn-diagram and table depicting the shared statistically significantly upregulated genes among four cephalosporin treatments after RNA-Seq analysis. (B) Annotations and fold-changes of the five shared statistically significantly upregulated loci among the four cephalosporin

Figure 2.5

Figure 2.5. Organization of coding sequences CD630_04570 through CD630_04620. Hp, hypothetical protein; aap, ABC transporter ATP-binding protein; atp, ABC transporter permease; hk, histidine kinase; rrtf, response regulator transcription factor.

2.7 Supplemental Information

Figure S1

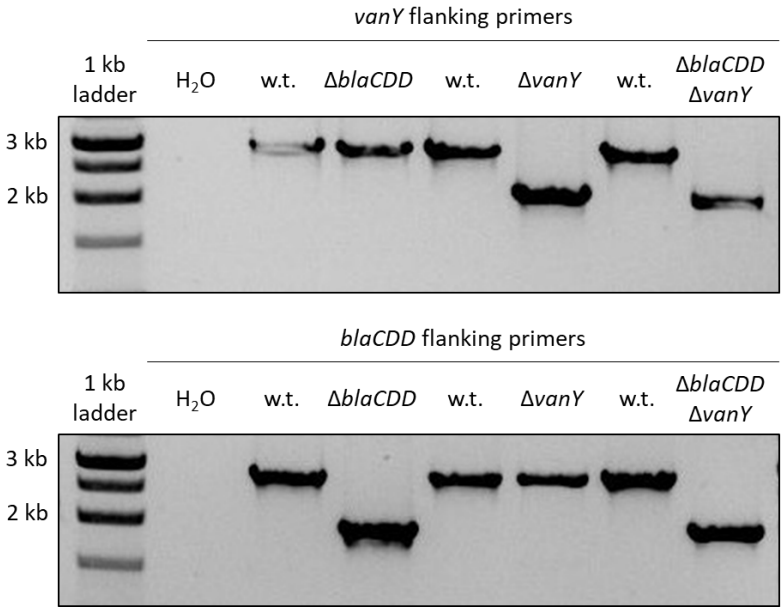

Figure S1. Confirmation of 630Δ*erm*Δ*pyrE* mutants using flanking primers. Isolated colonies of either 630 wildtype or 630Δ*erm*Δ*pyrE* mutants were inoculated into 100 µL of H_2O. The inocula were directly used for PCR using primers that flank either *blaCDD* or *vanY*. The absence of the gene of interest yields a band of lower molecular weight.

Table S1. Primers used for RT-qPCR analysis				
Locus tag	**Primer sequences**	**Amplicon (bp)**	**Tm (°C)**	**Reference**
CD630_00720 (*rpsJ)*	F: 5'-GATCACAAGTTTCAGGACCTG-3' R: 5'-GTCTTAGGTGTTGGATTAGC-3'	151	75.5	(85)
CD630_03440	F: 5'-GGTGGCACGAATACAGGAATA-3' R: 5'-CTCCTAGGTCTTGAACCACATAAC-3'	86	75	This study
CD630_04580 (*blaCDD*)	F: 5'-GGATGCATGGGTTGTTGGTATG-3' R: 5'-ACCTTTGGCCCTGTAATTTCT-3'	99	75.5	This study
CD630_04640	F: 5'-CCAGAAGGCTCATTAAGGATGT-3' R: 3'-CCTGGAGTATGACCAGGAGTAT-3'	92	74.2	This study
CD630_04700 (*blaR*)	F: 5'-CTGAAAGTACCAGTTTACGGAGT-3' R: 5'-ACATATCCCTTGGGATGGAAAG-3'	100	75	This study
CD630_04710 (*blaI*)	F: 5'-CTCTCAGTTCCTCAATATCATCTTC-3' R: 5'-ACGTAGCTACAGAAAGTAGTTC-3'	120	72.5	This study
CD630_05150	F: 5'-CCATCACCAAGTACAACACCTA-3' R: 5'-GCTGGATATTGCCTTGCATTT-3'	92	74.2	This study
CD630_05270	F: 5'-CATCAGTATGTCCTGGTGTATCT-3' R: 5'-CTTGTGTCTGACAAGAATCGTAAA-3'	79	72	This study
CD630_05480	F: 5'-ATCCCTTAGTTTGGGTGATGTT-3' R: 5'-CAGCCCTATATTCTTCACCAAGT-3'	99	72.5	This study
CD630_06550	F: 5'-CCTGCAATCTACACAGAAGATGA-3' R: 5'-CCGGAAGACCTGTGTCAATAAG-3'	52	73.5	This study
CD630_07810	F: 5'-CCTCCAGCTAGTGCTCTTATTT-3' R: 5'-CGCAAGCTGCAATGGTAATC-3'	61	72.6	This study
CD630_08290	F: 5'-GTACCCTTGTCACTGTGTTTCT-3' R: 5'-CAGCCCTACTCCAACTTCATTTA-3'	82	73.5	This study
CD630_08950	F: 5'-AAAGCAAGTACGAGAGTTCAAATG-3' R: 5'-CCTCTGCATCTCCTGCAAATA-3'	90	72.8	This study
CD630_11480	F: 5'-CCAGCAGATGACCCAGAAATAG-3' R: 5'-ACACTTGAATCACCTTGAGGAA-3'	58	73.5	This study
CD630_12290	F: 5'-CTAGGATTGGTACAGCTAAAGACC-3' R: 5'-AACTCCACAACCACCTTCAATA-3'	53	72	This study
CD630_12910	F: 5'-ATGCTGATGCCAACCAACTA-3' R: 5'-GTCCACTACCAACATCCATCAA-3'	66	73.5	This study
CD630_13740	F: 5'-AGGGACTACTCACTCGCA-3' R: 5'-CGCTTCCTAAGCCCAGTT-3'	89	76.5	This study
CD630_13990	F: 5'-GGCAGCAAATGTAGGTAAATGG-3' R: 5'-CCTCCCATTATTATTCCCTCTG-3'	150	73	This study
CD630_14060	F: 5'-GCCTACTGATGAACCTATAAGC-3' R: 5'-CTGGAGCTAGTTCACTGTTTAC-3'	116	73.5	This study
CD630_14690	F: 5'-GTTGACACAATCCCAACCTAAAC-3' R: 5'-GGCCTGAAGGAGAAGATTCTATAC-3'	56	72.5	This study
CD630_16270 (*vanY*)	F: 5'-GTTCTCTGCGTGACAATGGA-3' R: 5'-AATAGCAAGCCCTGTCTGATG-3'	86	76	This study
CD630_18020	F: 5'-CGTAGATGGTAAGGATGC-3' R: 5'-TCCTCCTATATGGTCTGC-3'	142	73.2	This study
CD630_21410	F: 5'-CCTGTTTCTTGGTCTATAAG-3' R: 5'-CATTAGCCATGATTCTAGTT-3'	106	72.1	This study

CD630_24980	F: 5'-TGTTGGTGGTGGCAATGTA-3' R: 5'-GCCTCAGAGTTCATTAGGTGAA-3'	51	72	This study
CD630_25040	F: 5'-TCAGCTAAACCTGGAGAGAGT-3' R: 5'-CCCAACAAGACTGGTCATCTC-3'	76	76.5	This study
CD630_26560	F: 5'-CTGAAGGTGGAGGAAAGATAGC-3' R: 5- CCTGGAGCATACTTACCATCTATAAC-3'	97	74.5	This study
CD630_27420	F: 5'-CCTATATGGTCTCCATGC-3' R: 5'-CCCAGGTGGAAGTTTAG-3'	99	72.5	This study
CD630_29630	F: 5'-CACCTGTAAGTTATTGGCTTCC-3' R: 5'-CATCCATGTGAACCTGAAGAC-3'	109	75	This study
CD630_30070	F: 5'-CAGTAAGCGAATATGCTTGGAG-3' R: 5'-TGAAGGACTTCAACCCTAGA-3'	106	73.5	This study
CD630_31960	F: 5'-CTCCAGTTCCCATTGCTGAATA-3' R: 5'-CGGTTATCTGTGGTGGCTATG-3'	65	74.5	This study
CD630_36010	F: 5'-AAACAAATGGCAGGAGAACC-3' R: 5'-GATCTGTATGCTGAAGACCCTA-3'	98	76	This study
CD630_36510	F: 5'-AGGGAGTGGTAGTAGTGGTAAT-3' R: 5'-GCCACTTAATCCTGCATCTACT-3'	79	72.4	This study

Table S2

Table S2. Primers used for molecular cloning. Bases in bold are restriction sites			
Designation	**Application**	**Primer sequence**	**Reference**
A1	04580 upstream homology (BamHI) FWD	5'-**GGATCC**TAAATAAAGAATAAATAATTACCTCAC-3'	This study
A2	04580 upstream homology (XbaI) REV	5'-**TCTAGA**AGCTACAACAACTAGAAGAATAAC-3'	This study
B1	04580 downstream homology (XbaI) FWD	5'-**TCTAGA**ACTTAATTTTATTTGTAAATATTATTTACC-3'	This study
B2	04580 downstream homology (NotI) REV	5'-**GCGGCCGC**ACAAGTCTACAATTTCTTCTGAAT-3'	This study
C1	04580 flanking FWD	5'-GATATATTCTGCTATGTTATAGAAGGTATTTC-3'	This study
C2	04580 flanking REV	5'-CTCATCATGAGTAATAAGAAGTATTGTC-3'	This study
D1	04580 internal sequence FWD	5'-GATAGATAAAGTTGATGCTAAATCTGTCC-3'	This study
E1	16270 flanking FWD	5'-GCAGTTATATTTGGTGGAAACTCAACAG-3'	This study
E2	16270 flanking REV	5'-GGTATTTACCTTATGTTCTCCTTTCAAGTC-3'	This study
F1	16270 internal FWD	5'-GGGTTAAAGAAAGAAGTTATAGATTTTATC-3'	This study
G1	Gibson: 16270 upstream homology FWD	5'-AATTGTTCAAAAAAATAATGGCGGCGCGCCGGATGTGGTACTCTTTCTTCAGCATTATGT-3'	This study
G2	Gibson: 16270 upstream homology REV	5'-CAAGGCAAGACCGATCGGGCCCCCTGCAGGCCCCTAGTTTATGTAAAAACATTCCCTCAC-3'	This study
H1	Gibson: 16270 SOE FWD	5'-GACAAGATAATTGAGGTGTACATAAAATGAAGGACTAAGAAATGGAGGAACAAGAATGA-3'	This study
H2	Gibson: 16270 SOE REV	5'-TCATTCTTGTTCCTCCATTTCTTAGTCCTTCATTTTATGTACACCTCAATTATCTTGTC-3'	This study

I1	Δ04580 Sanger sequencing FWD	5'-GATTTTATAAATAGAAGTATTCAAGCTCC-3'	This study
I2	Δ04580 Sanger sequencing FWD	5'-CATAGTCTTTAAAAGGTATTAACTTTAAATC-3'	This study
J1	Δ16270 Sanger sequencing FWD	5'-GCTAGAATTGATTTGGATTGTGAGA-3'	This study
J2	Δ16270 Sanger sequencing REV	5'-AAAGAATGGCACAGCAATACG-3'	This study
K1	rpsJ (310 bp) FWD	5'-ATGGCTAAGAATGAAAAAATAAGAATAAGA-3'	This study
K2	rpsJ (310 bp) REV	5'-ATAATTTTATTTCTATATCTACACCTGCTG-3'	This study
L1	rrs (120 bp) FWD	5'-GGGAGACTTGAGTGCAGGAG-3'	(85)
L2	rrs (120 bp) REV	5'-GTGCCTCAGCGTCAGTTACAGT-3'	(85)

Table S3

Table S3. Relative normalized expression and regulation of qPCR analyses

Locus tag	w.t. RNE Ratio	w.t. Regulation Change	w.t. P-value	ΔblaCDD RNE Ratio	ΔblaCDD Regulation Change	ΔblaCDD P-value	ΔblaCDD/ w.t. Fold-Change
03440	1.7	NC	0.008584	1.3	NC	0.001869	0.8
04580	577.1	Upreg.	0.000005	N/A	N/A	N/A	N/A
04640	2.0	NC	0.000344	1.9	NC	0.001552	1.0
04700	2.3	NC	0.015522	4.0	Upreg.	0.000000	1.7
04710	3.0	NC	0.000459	6.8	Upreg.	0.000253	2.3
05150	1.0	NC	0.761605	0.9	NC	0.483523	0.9
05270	0.6	NC	0.016299	1.5	NC	0.003926	2.6
05480	1.5	NC	0.009281	2.3	NC	0.001221	1.5
06550	2.1	NC	0.002291	4.1	Upreg.	0.000085	2.0
07810	2.1	NC	0.000449	2.4	NC	0.003191	1.1
08290	1.5	NC	0.045882	2.7	NC	0.003940	1.8
08950	0.7	NC	0.011207	1.5	NC	0.007136	2.1
11480	3.2	NC	0.000066	3.2	NC	0.001048	1.0
12290	1.9	NC	0.021594	0.9	NC	0.212311	0.5
12910	1.0	NC	0.773211	0.9	NC	0.426972	0.9
13740	1.3	NC	0.004840	1.1	NC	0.375541	0.8
13990	1.1	NC	0.506512	3.4	NC	0.001130	3.1
14060	2.1	NC	0.008106	2.2	NC	0.001288	1.0
14690	0.8	NC	0.231887	1.5	NC	0.044871	1.9
16270	9.6	Upreg.	0.000038	15.6	Upreg.	0.001615	1.6
18020	1.6	NC	0.032620	3.0	NC	0.001210	1.9
21410	1.8	NC	0.263273	1.3	NC	0.161863	0.7
24980	1.1	NC	0.647770	1.3	NC	0.361777	1.2
25040	2.7	NC	0.000031	3.4	NC	0.000495	1.3
26560	0.5	NC	0.019257	2.3	NC	0.000909	4.6
27420	2.0	NC	0.109910	1.6	NC	0.001761	0.8
29630	1.0	NC	0.949294	1.8	NC	0.001097	1.8
30070	1.6	NC	0.018557	2.1	NC	0.002581	1.3
31960	0.8	NC	0.008535	1.9	NC	0.002397	2.4
36010	2.4	NC	0.001271	7.0	Upreg.	0.000069	2.9
36510	0.6	NC	0.001532	1.1	NC	0.288971	1.8

A 4-fold change in expression was deemed as “upregulated” according to the default settings in CFX Manager. Biological samples n=1/treatment, P-value reported is from technical replicates n=3/plate. NC, no change; Upreg., upregulated; w.t., 630 wildtype; RNE, relative normalized expression. The “CD630” prefix of the locus tags were removed due to space constraints in the table. Red cells, P>0.01; gray cells, P<0.01; blue cells, P<0.001.

Table S4

Table S4. KEGG Orthology (KO) identifiers that are differentially expressed in metabolic and environmental information processing pathways.

		Number of differentially expressed KOs							
General Category	**Pathway**	**CPR**		**CFX**		**CFT**		**CFP**	
		U	**D**	**U**	**D**	**U**	**D**	**U**	**D**
Metabolism	Metabolic pathways	4	8	90	24	20	16	0	0
	Biosynthesis of secondary metabolites	2	4	31	6	8	8	0	0
	Microbial metabolism in diverse environments	1	4	21	3	5	5	0	0
	Carbon metabolism	0	5	12	4	1	4	0	0
	2-Oxocarboxylic acid metabolism	0	0	4	0	0	1	0	0
	Fatty acid metabolism	0	1	1	0	0	0	0	0
	Biosynthesis of amino acids	0	1	17	3	4	6	0	0
	Degradation of aromatic compounds	0	0	0	1	0	0	0	0
Environmental Information Processing	ABC transporters	7	5	19	6	11	3	1	4
	Phosphotransferase system (PTS)	1	0	18	7	5	2	0	0
	Bacterial secretion system	1	0	0	0	1	0	0	0
	Two-component system	0	1	9	5	2	6	0	2

Names for General Categories and Pathways are listed as in the KEGG database. The number of upregulated and downregulated KO identifiers are from genes with a greater than 2-fold change in expression and an FDR cut-off of $P < 0.05$. U: upregulated; D: downregulated; CPR: cephradine; CFX: cefoxitin; CFT: ceftazidime; CFP: cefepime

CHAPTER 3: Future Directions

In this thesis, we identified the upregulation of a putative ß-lactamase, *blaCDD*, and a putative D,D-carboxypeptidase, *vanY*, upon cefoxitin exposure. Upon deletion of *blaCDD* and *vanY*, both individually and together, we saw minimal to no change in the cephalosporin susceptibility of *C. difficile* strain 630. Global transcriptomic analysis of *C. difficile* strain 630 upon exposure to four cephalosporins revealed the shared significant upregulation of a putative heterodimeric ABC transporter encoded by two overlapping loci (CD630_04590 and CD630_04600). Our future work will be geared towards elucidating the role of these two loci in cephalosporin resistance. We will also pursue a global genomic mutational analysis to detect other genes essential for cephalosporin resistance.

Heterodimeric ABC transporters are composed of two separate polypeptide monomers: an ATP-binding subunit that contains nucleotide-binding domains and a permease subunit that contains transmembrane domains. Both the ATP-binding and the permease subunits must be present in order to create a functional transporter. The importance of both subunits was highlighted for the DrrAB transporter within *Streptomyces peucetius* (67). Moreover, deletion of the permease component of the heterodimeric transporter AnrAB in *Listeria monocytogenes* effectively increased susceptibility to ß-lactam antibiotics and other drugs (69).

We will begin by individually deleting each subunit of the CD630_04590/CD630_04600 ABC transporter, and testing the minimum inhibitory concentration (MIC) of the resulting mutants for the four cephalosporins used in this thesis. We hypothesize that deleting either the ATP-binding protein or the transmembrane permease will abolish the transporter's activity and decrease *C. difficile*'s resistance to cephalosporins.

If we observe that the heterodimer ABC transporter is indeed required for cephalosporin resistance, we will confirm the activity of CD630_04590/CD630_04600 by heterologous expression in *Escherichia coli* and measure increased drug resistance. We will also use inverted membrane vesicles to measure efflux activity (68, 109).

If we observe that deleting either gene CD_04590 or CD_04600 do not affect cephalosporin resistance, it could be that the monomer is associating with a monomer expressed by another transporter. Indeed, a cursory look at the *C. difficile* strain 630 genome using search terms "ABC-type transport system, permease" and "ABC-type transport system, ATP-binding protein" reveals the following: 23 putative heterodimeric ABC ATPase/permease pairs, one operon comprising of a permease and fragment of an ATPase, two operons with one ATPase and two permeases, one operon with two ATPases and one permease, and finally, six orphan ATPases. These ABC transporters are suggested to be involved in transport of sugars, amino acids, cations and other metabolites. Of course, a detailed BLAST search will be necessary to better reveal the true number of putative heterodimeric ABC transporters, as there could be others annotated with other names. Although this mechanism would be interesting, interaction between subunits from different heterodimeric ABC transporters has not, to our knowledge, yet been reported in the literature.

If deletion of either the CD630_04590 ATP binding protein or the CD630_04600 permease does not affect cephalosporin resistance, we will also delete both subunits of the ABC transporter simultaneously. If we observe a drastic decrease in the MICs for this mutant, this suggests that this ABC transporter is functional in providing cephalosporin resistance but that at least one of the subunits must interact with other heterodimeric ABC transporters.

If we do not observe substantial decreases in cephalosporin resistance for either the ΔCD630_04590, ΔCD630_04600 single mutants or the ΔCD630_04590ΔCD630_04600 double mutant, it could be that 1) these two loci encode a nonfunctional protein or 2) the heterodimer ABC transporter is involved in other functions not related to antibiotic resistance. Both scenarios would suggest that there are other genes responsible for cephalosporin resistance.

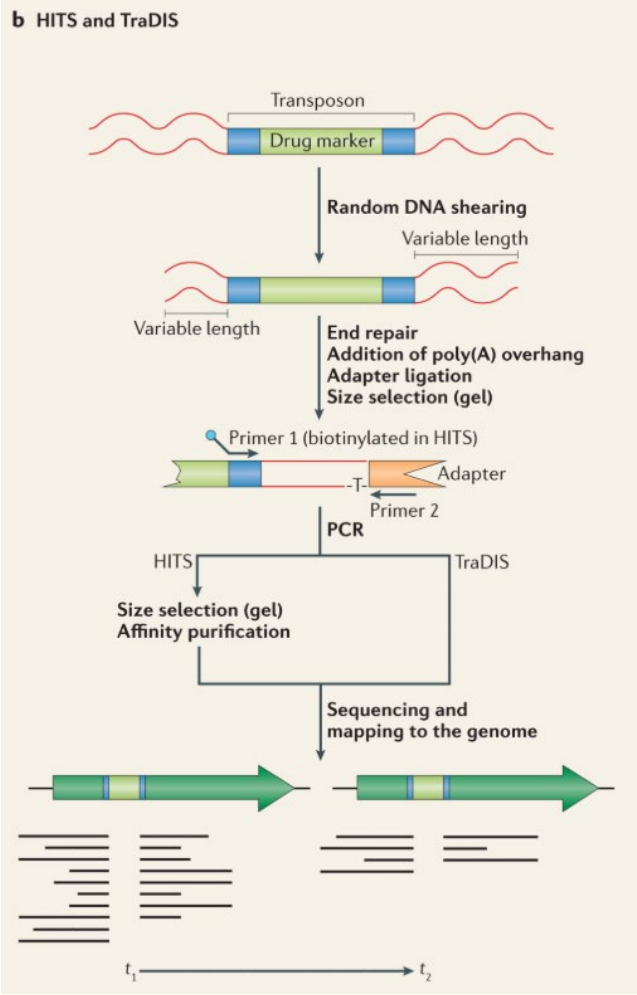

Figure 3.1. TraDIS schematic. Adapted from van Opijnen & Camilli (2013).

In order to further elucidate genes that are essential for cephalosporin resistance, but are constitutively expressed regardless of antibiotic exposure, our next strategy will be to use Transposon Directed Insertion Sequencing (TraDIS). This method has already been used to study *C. difficile* strain R20291 to identify genes essential for *in vitro* growth and sporulation (110).

For our future study, we will create a *mariner* transposon library consisting of at least 10^5 transposon mutants of *C. difficile* strain 630. This density of insertions will ensure that every gene of the *C. difficile* strain 630 genome is deleted in at least one member of the population.

The resulting library will be grown in the presence and absence of cefoxitin. Both populations will be harvested, lysed and their genome fragmented through random DNA shearing (**Figure 3.1**) (111). Transposon-containing fragments will then be PCR-amplified and Illumina-sequenced. We expect that the comparison of gene sequence densities in the treated vs. untreated populations (t_1 vs t_2) will allow the determination of genes that were targeted by transposon mutagenesis and are required for cephalosporin resistance.

APPENDIX

EQUATIONS A1 – A3

$$E = 10^{-1/slope}$$

Equation A1. qPCR Efficiency calculation. *Slope* is given by the standard curve. E: efficiency

---

$$Relative\ normalized\ expression\ ratio = \frac{E_{tar}^{\Delta Cq_{tar}(control-treated)}}{E_{ref}^{\Delta Cq_{ref}(control-treated)}}$$

Equation A2. Relative normalized expression (RNE) ratio calculation. E: efficiency; Cq: quantification (or threshold) cycle; tar: target; ref: reference

---

$$Regulation = \frac{-1}{RNE\ ratio}$$

Equation A3. Regulation calculation. RNE: relative normalized expression

---

Figure A1

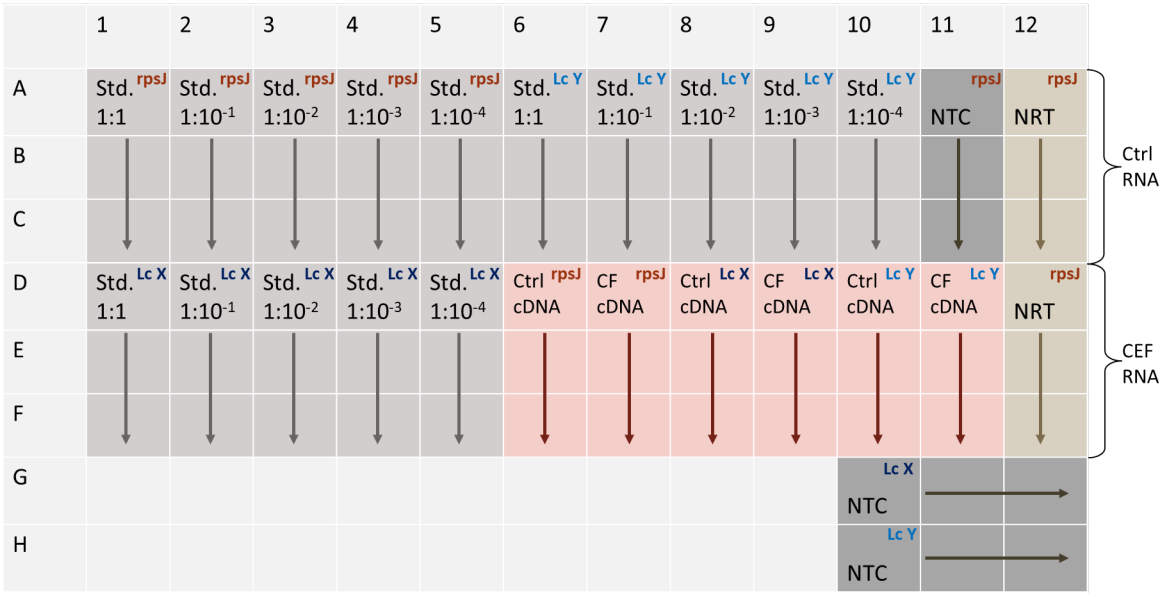

Figure A1. qPCR plate set-up. Std: standard; Ctrl: control (untreated); CF/CEF: cefoxitin; NTC: no template control; NRT: no reverse transcription control; Lc X: locus X; Lc Y: locus Y

Table A1

Table A1. Nanodrop values pre-DNase treatment

Sample	ng/µL	A260/A280	A260/A230
ΔblaCDD ctrl RNA #1	218.1	2.3	2.3
ΔblaCDD ctrl RNA #2	206.5	2.2	2.2
ΔblaCDD ctrl RNA #3	238.3	2.2	2.5
ΔblaCDD cfx RNA #1	206.4	2.1	1.5
ΔblaCDD cfx RNA #2	221.8	2.1	2.4
ΔblaCDD cfx RNA #3	224.6	2.1	2.2
wildtype ctrl RNA #1	294.2	2.1	2.4
wildtype ctrl RNA #2	217.3	2.1	2.0
wildtype cfx RNA #1	192.1	2.1	2.3
wildtype cfx RNA #2	284.7	2.1	2.4
ctrl 1	572.0	2.2	2.2
ctrl 2	689.5	2.2	2.2
ctrl 2-2	51.8	2.6	1.4
ctrl 3	613.4	2.1	2.3
A 1	58.3	2.1	1.3
A 2	406.2	2.8	2.4
A 3	340.3	2.1	2.0
B 1	119.6	2.2	1.6
B 1-2	72.5	2.2	0.4
B 2	85.3	2.1	1.9
B 2-2	73.4	2.4	0.9
B 3	101.6	2.1	1.9
B 3-2	80.9	2.5	1.1
C 1	306.1	2.1	1.7
C 2	230.1	2.1	2.3
C 3	350.0	2.1	2.5
D 1	220.3	2.1	2.0
D 2	275.7	2.1	2.4
D 3	282.2	2.1	2.1

Yellow highlighted samples are those used for qPCR analyses. Number designations for qPCR samples indicate technical replicates and derived from one biological sample. Unhighlighted samples are wildtype samples used for RNA-Seq analyses. Number designations indicate biological replicates. Values highlighted in red are A260/A230 values that fall below 1.5.

Table A2

Table A2. Nanodrop values post-DNase treatment and ethanol precipitation prep.

Sample	ng/µL	A260/A280	A260/A230
ΔblaCDD ctrl RNA #1	148.2	2.0	2.5
ΔblaCDD ctrl RNA #2	115.3	2.1	2.7
ΔblaCDD ctrl RNA #3	162.1	2.0	2.7
ΔblaCDD cfx RNA #1	149.9	2.0	2.6
ΔblaCDD cfx RNA #2	148.7	2.0	2.5
ΔblaCDD cfx RNA #3	161.5	2.0	2.7
wildtype ctrl RNA #1	228.9	2.0	2.6
wildtype ctrl RNA #2	163.0	2.0	2.7
wildtype cfx RNA #1	138.2	2.0	2.6
wildtype cfx RNA #2	187.8	2.1	2.5
ctrl 1	272.1	2.0	2.7
ctrl 2	255.3	2.0	2.7
ctrl 2-2	86.6	1.8	1.5
ctrl 3	250.8	2.1	2.6
A 1	73.6	2.3	2.2
A 2	291.0	2.0	2.6
A 3	242.5	2.0	2.6
B 1	68.2	2.0	2.0
B 1-2	107.1	2.0	2.2
B 2	84.5	2.1	2.2
B 2-2	92.9	1.9	2.3
B 3	99.8	2.0	2.4
B 3-2	127.5	2.0	2.3
C 1	269.2	2.1	2.7
C 2	240.2	2.1	2.5
C 3	261.7	2.0	2.6
D 1	262.8	2.0	2.6
D 2	257.4	1.9	1.8
D 3	244.5	2.0	2.6

Yellow highlighted samples are those used for qPCR analyses. Number designations for qPCR samples indicate technical replicates and derived from one biological sample. Unhighlighted samples are wildtype samples used for RNA-Seq analyses. Number designations indicate biological replicates. Blue highlighted samples are those that were concentrated using the CentriVap.

Figure A2

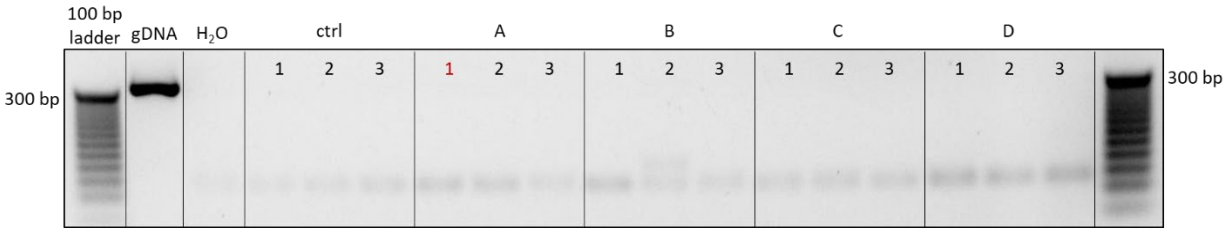

Figure A2. gDNA contamination check on RNA-Seq samples collected during late exponential phase. Primers used were K1 and K2 (refer to Table S2). The sample in red was found to have a low RIN value, and was replaced by another A1 sample later on.

Figure A3

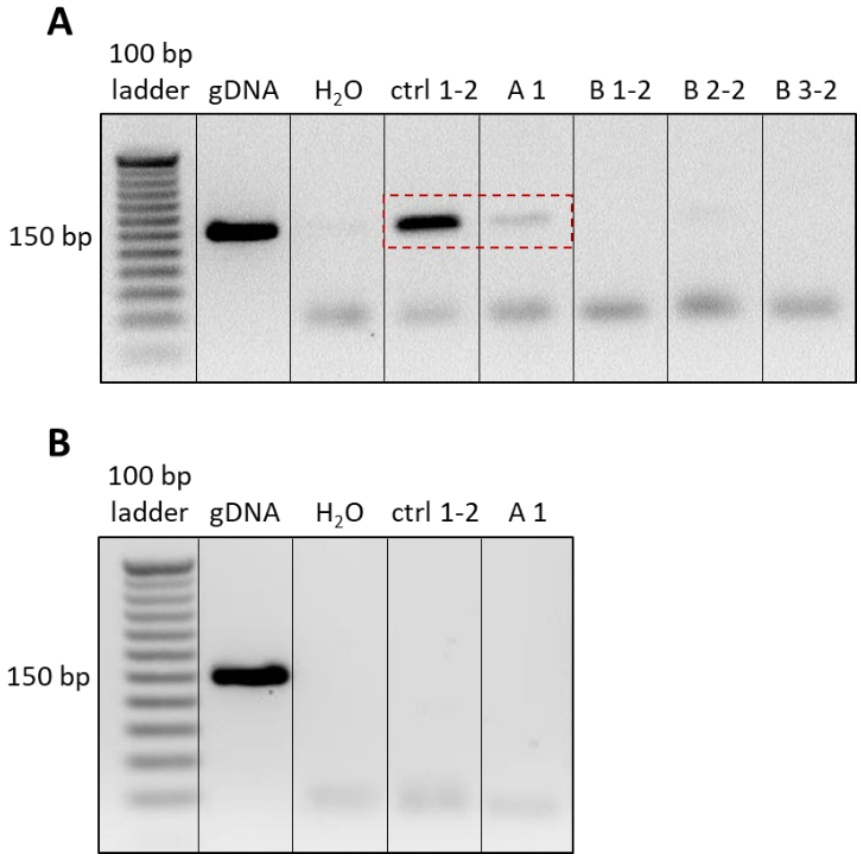

Figure A3. gDNA contamination check on RNA-Seq samples re-collected a mid-exponential phase. (A) Agarose gel depicting the presence or absence of gDNA contamination in RNA samples after using RNA as PCR template. Band boxed in red indicates slight gDNA contamination. (B) gDNA contamination check on samples after three rounds of DNase-treatment. Primers used were against *rpsJ* from Table S1.

Figure A4

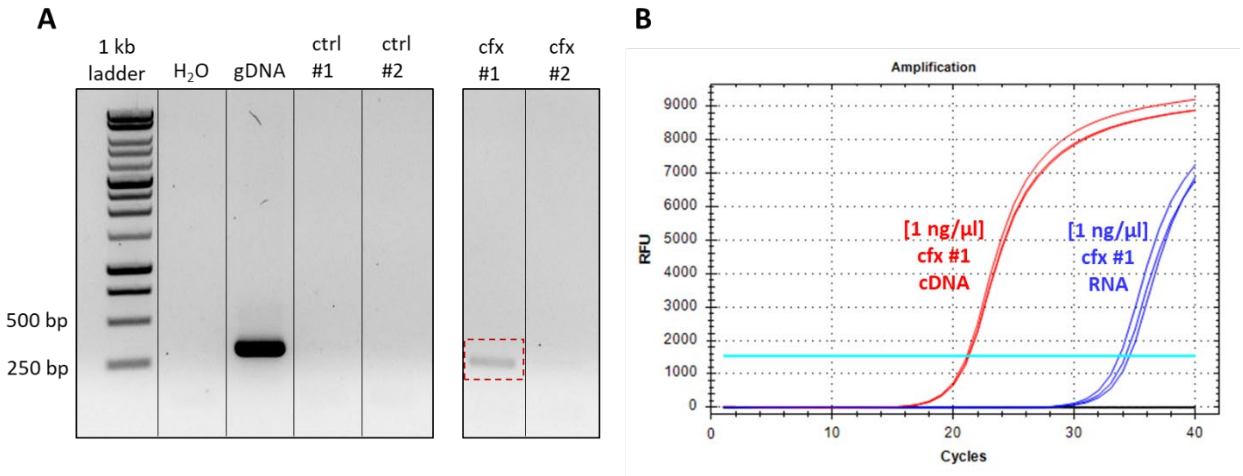

Figure A4. gDNA contamination check on *C. difficile* strain 630 wildtype samples for qPCR analysis. (A) Agarose gel depicting the presence or absence of gDNA contamination in RNA samples after using RNA as PCR template. Band boxed in red indicates slight gDNA contamination. Primers used were K1 and K2 in Table S2. (B) Quantification of gDNA contamination using an NRT control of the contaminated RNA (in blue) against a cDNA sample reverse-transcribed from the contaminated RNA.

Figure A5

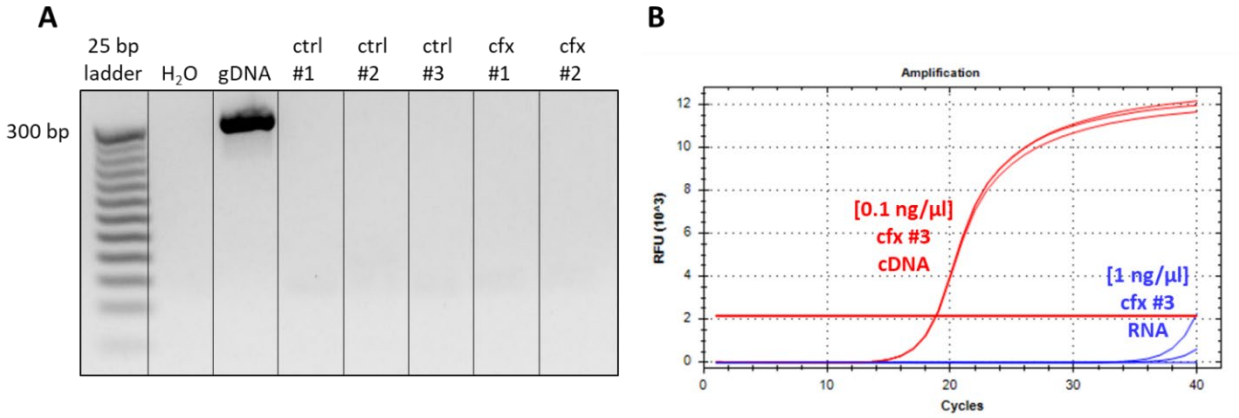

Figure A5. gDNA contamination check on *C. difficile* strain 630ΔermΔpyrEΔblaCDD samples for qPCR analysis. (A) Agarose gel depicting the presence or absence of gDNA contamination in RNA samples after using RNA as PCR template. Primers used were K1 and K2 in Table S2. (B) Quantification of gDNA contamination using an NRT control of RNA sample "cfx #3" (in blue) against a cDNA sample reverse-transcribed from the RNA samples "cfx #3".

Table A3

Table A3. Bioanalyzer RNA Integrity Values (RINs)				
Sample	**Rep. 1**	**Rep. 2**	**Rep. 3**	**Avg.**
ΔblaCDD ctrl RNA #1	9.5	N/A	N/A	9.5
ΔblaCDD ctrl RNA #2	10.0	10.0	N/A	10.0
ΔblaCDD ctrl RNA #3	10.0	10.0	N/A	10.0
ΔblaCDD cfx RNA #1	9.9	9.9	N/A	9.9
ΔblaCDD cfx RNA #2	10.0	10.0	N/A	10.0
ΔblaCDD cfx RNA #3	10.0	10.0	N/A	10.0
wildtype ctrl RNA #1	8.0	8.5	N/A	8.3
wildtype ctrl RNA #2	7.9	N/A	N/A	7.9
wildtype cfx RNA #1	8.9	N/A	N/A	8.9
wildtype cfx RNA #2	9.1	N/A	N/A	9.1
ctrl 1	9.2	N/A	N/A	9.2
ctrl 2	9.6	N/A	N/A	9.6
ctrl 2-2	9.7	9.6	9.7	9.7
ctrl 3	9.8	N/A	N/A	9.8
A 1	N/A	10.0	9.8	9.9
A 2	9.7	N/A	N/A	9.7
A 3	9.8	N/A	N/A	9.8
B 1	10.0	N/A	N/A	10.0
B 1-2	9.9	N/A	N/A	9.9
B 2	9.9	N/A	N/A	9.9
B 2-2	9.9	N/A	N/A	9.9
B 3	9.2	N/A	N/A	9.2
B 3-2	9.6	N/A	N/A	9.6
C 1	9.8	N/A	N/A	9.8
C 2	9.7	N/A	N/A	9.7
C 3	9.9	N/A	N/A	9.9
D 1	9.8	N/A	N/A	9.8
D 2	9.9	N/A	N/A	9.9
D 3	9.7	N/A	N/A	9.7

"N/A" written in black indicate the absence of a technical replicate. "N/A" highlighted in red indicate technical replicates in which no RIN value was produced, but that the electrophoretogram itself was satisfactory.

Figure A6

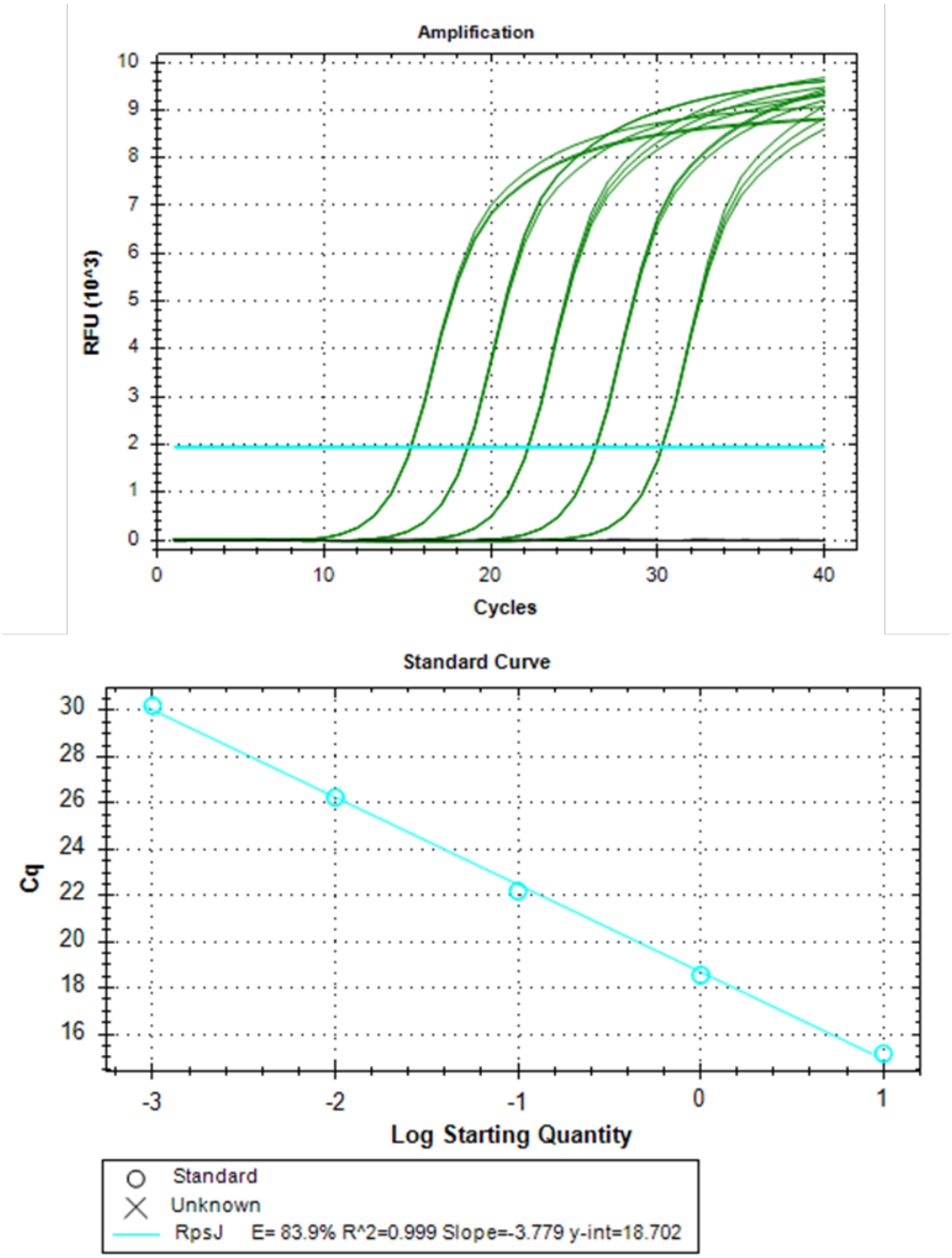

Figure A6. RpsJ qPCR primers amplification plot and standard curve. A 5-point serial dilution of gDNA was used to calculate the efficiency of qPCR primers. Green amplification curves are standard curves, whereas black amplification curves are no template controls (NTCs). Each dilution was run in technical triplicate.

Table A4

Table A4. qPCR primer efficiencies

qPCR Primers	Efficiency	R^2
CD630_00720 (*rpsJ)*	84.0	0.996
CD630_03440	81.8	0.996
CD630_04580 (*blaCDD*)	87.6	0.998
CD630_04640	79.4	0.994
CD630_04700 (*blaR*)	82.2	0.996
CD630_04710 (*blaI*)	85.6	0.998
CD630_05150	84.6	0.998
CD630_05270	84.2	0.999
CD630_05480	86.0	0.998
CD630_06550	84.6	0.998
CD630_07810	81.1	0.998
CD630_08290	88.5	0.998
CD630_08950	82.1	0.996
CD630_11480	83.6	0.998
CD630_12290	88.8	0.995
CD630_12910	83.8	0.999
CD630_13740	86.5	0.998
CD630_13990	81.2	0.997
CD630_14060	89.2	0.996
CD630_14690	82.0	0.996
CD630_16270 (*vanY*)	83.5	0.996
CD630_18020	82.6	0.987
CD630_21410	74.0	0.990
CD630_24980	88.8	0.996
CD630_25040	87.0	0.998
CD630_26560	84.8	0.996
CD630_27420	70.5	0.991
CD630_29630	88.4	0.996
CD630_30070	87.4	0.995
CD630_31960	85.0	0.998
CD630_36010	76.1	0.994
CD630_36510	78.2	0.997

Efficiencies were calculated using *C. difficile* strain 630 genomic DNA as template for each standard curve. Standard curves were run in technical triplicates per 96-well plate. Efficiencies and R^2 values are the average of at least two independent qPCR runs.

Figure A7

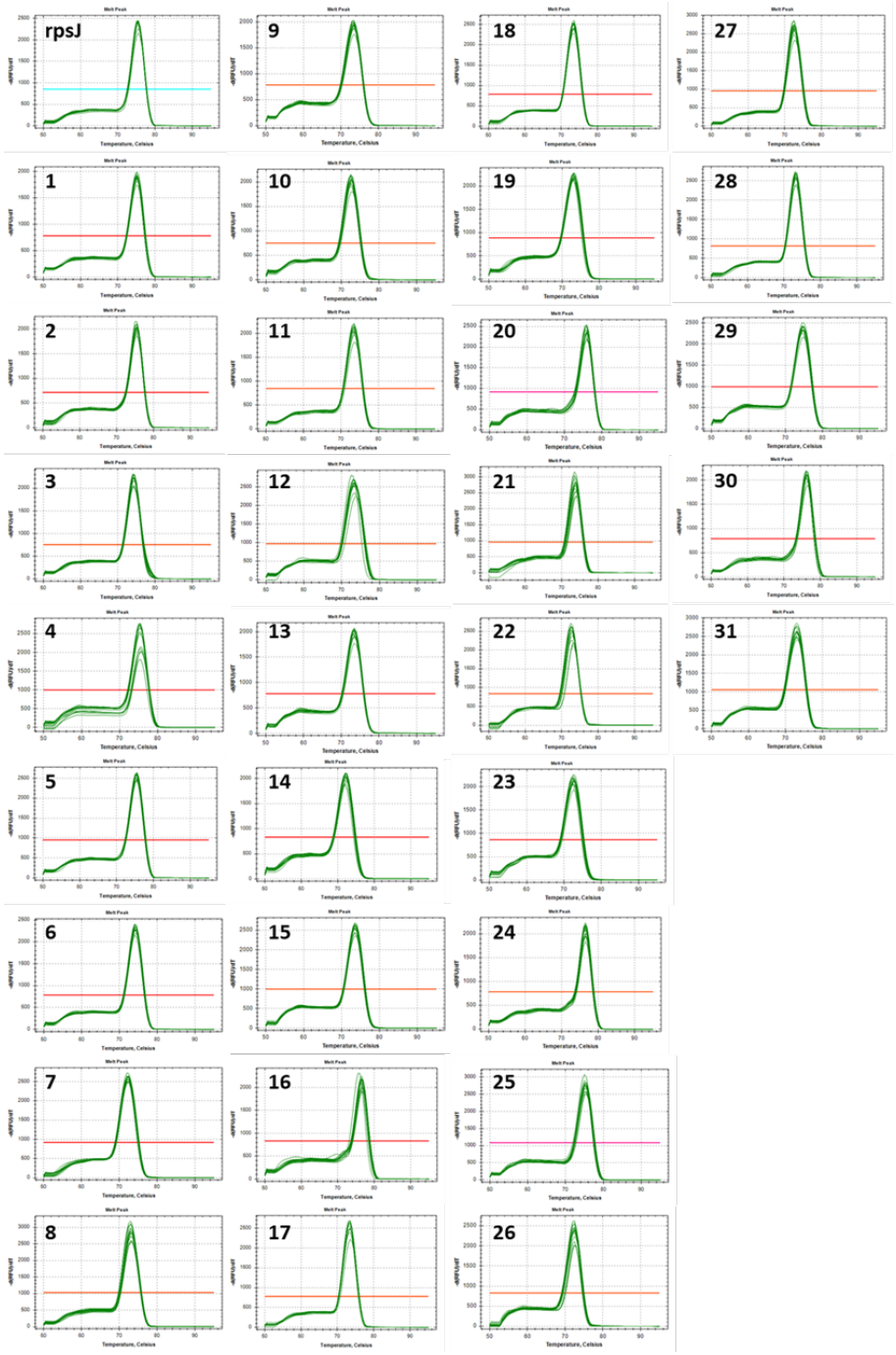

Figure A7. Melting curve analysis of each primer set used for qPCR assays. Each graph plots the derivative of the melting curve on the Y-axis, and the temperature (°C) on the X-axis. The peaks represent the temperature at which half of the amplicons have disassociated into ssDNA.

REFERENCES

1. Hall IC, O'Toole E. 1935. Intestinal Flora in New-Born Infants - with a Description of a New Pathogenic Anaerobe, Bacillus difficilis. Am J Dis Child 49:390–402.

2. Voth DE, Ballard JD. 2005. Clostridium difficile Toxins: Mechanism of Action and Role in Disease. Clin Microbiol Rev 18:247–263.

3. Just I, Wilm M, Selzer J, Rex G, Von Eichel-Streiber C, Mann M, Aktories K. 1995. The enterotoxin from Clostridium difficile (ToxA) monoglucosylates the Rho proteins. J Biol Chem 270:13932–13936.

4. Just I, Selzer J, Wilm M, Von Eichel-Streiber C, Mann M, Aktories K. 1995. Glucosylation of Rho proteins by Clostridium difficile toxin B. Nature 375:500–503.

5. Bartlett JG, Moon N, Chang W, Taylor N, Onderdonk AB. 1978. Role of Clostridium difficile in Antibiotic-associated Pseudomembranous Colitis. Gastroenterology 75:778–782.

6. Spigaglia P. 2016. Recent advances in the understanding of antibiotic resistance in *Clostridium difficile* infection. Ther Adv Infect Dis 3:23–42.

7. Peng Z, Jin D, Kim HB, Stratton CW, Wu B, Tang Y-W, Sun X. 2017. Update on Antimicrobial Resistance in Clostridium difficile: Resistance Mechanisms and Antimicrobial Susceptibility Testing. J Clin Microbiol 55:1998–2008.

8. Miller BA, Chen LF, Sexton DJ, Anderson DJ. 2011. Comparison of the Burdens of Hospital-Onset, Healthcare Facility-Associated Clostridium difficile Infection and of Healthcare-Associated Infection due to Methicillin-Resistant Staphylococcus aureus in Community Hospitals. Infect Control Hosp Epidemiol 32:387–390.

9. Lessa FC, Mu Y, Bamberg WM, Beldavs ZG, Dumyati GK, Dunn JR, Farley MM, Holzbauer SM, Meek JI, Phipps EC, Wilson LE, Winston LG, Cohen JA, Limbago BM, Fridkin SK, Gerding DN, McDonald LC. 2015. Burden of *Clostridium difficile* Infection in the United States. N Engl J Med 372:825–834.

10. Desai K, Gupta SB, Dubberke ER, Prabhu VS, Browne C, Mast TC. 2016. Epidemiological and economic burden of Clostridium difficile in the United States: estimates from a modeling approach. BMC Infect Dis 16:303.

11. Centers for Disease Control and Prevention. 2019. Antibiotic Resistance Threats in the United States, 2019. Atlanta, GA.

12. Galperin MY. 2013. Genome Diversity of Spore-Forming Firmicutes. Microbiol Spectr 1: TBS-0015-2012.

13. Wells CL, Wilkins TD. 1996. Clostridia: Sporeforming Anaerobic Bacilli, p. 1012–1045. *In* Baron, S (ed.), Medical Microbiology, 4th ed. Galveston, TX.

14. Lawson PA, Citron DM, Tyrrell KL, Finegold SM. 2016. Reclassification of Clostridium difficile as Clostridioides difficile (Hall and O'Toole 1935) Prévot 1938. Anaerobe 40:90-95.

15. Lawson PA, Rainey FA. 2016. Proposal to restrict the genus Clostridium Prazmowski to Clostridium butyricum and related species. Int J Syst Evol Mcrobiology 66:1009–1016.

16. Oren A, Rupnik M. 2018. Clostridium difficile and Clostridioides difficile: Two validly published and correct names. Anaerobe 52:125–126.

17. Leffler DA, Lamont T. 2015. Clostridium difficile Infection. N Engl J Med 372:1539–1548.

18. Isidro J, Mendes AL, Serrano M, Henriques AO, Oleastro M. 2017. Overview of Clostridium difficile Infection: Life Cycle, Epidemiology, Antimicrobial Resistance and Treatment, p. 4–56. *In* Enany, S (ed.), Clostridium Difficile - A Comprehensive Overview. InTech, Egypt.

19. Lessa FC, Gould C V., Clifford McDonald L. 2012. Current status of clostridium difficile infection epidemiology. Clin Infect Dis 55:S65–S70.

20. Lawley TD, Clare S, Walker AW, Goulding D, Stabler RA, Croucher N, Mastroeni P, Scott P, Raisen C, Mottram L, Fairweather NF, Wren BW, Parkhill J, Dougan G. 2009. Antibiotic treatment of Clostridium difficile carrier mice triggers a supershedder state, spore-mediated transmission, and severe disease in immunocompromised hosts. Infect Immun 77:3661–3669.

21. Lessa FC, Mu Y, Bamberg WM, Beldavs ZG, Dumyati GK, Dunn JR, Farley MM, Holzbauer SM, Meek JI, Phipps EC, Wilson LE, Winston LG, Cohen JA, Limbago BM, Fridkin SK, Gerding DN, Mcdonald LC. 2015. Burden of Clostridium difficile Infection in the United States. N Engl J Med 372:825–834.

22. Di Bella S, Gouliouris T, Petrosillo N. 2015. Fecal microbiota transplantation (FMT) for Clostridium difficile infection: Focus on immunocompromised patients. J Infect Chemother 21:230–237.

23. Wilcox MH, Chalmers JD, Nord CE, Freeman J, Bouza E. 2017. Role of cephalosporins in the era of Clostridium difficile infection. J Antimicrob Chemother 72:1–18.

24. Slimings C, Riley T V. 2014. Antibiotics and hospital-acquired Clostridium difficile infection: Update of systematic review and meta-analysis. J Antimicrob Chemother 69:881–891.

25. Brown KA, Khanafer N, Daneman N, Fisman DN. 2013. Meta-Analysis of Antibiotics and the Risk of Community-Associated Clostridium difficile Infection. Antimicrob Agents Chemother 57:2326–2332.

26. Loo VG, Poirier L, Miller MA, Oughton M, Libman MD, Michaud S, Bourgault A-M, Nguyen T, Frenette C, Kelly M, Vibien A, Brassard P, Fenn S, Dewar K, Hudson TJ, Horn R, René P, Monczak Y, Dascal A, Maisonneuve-Rose-mont H, de Montréal UL, Mortimer Davis-Jewish SB. 2005. A Predominantly Clonal Multi-Institutional Outbreak of Clostridium difficile-Associated Diarrhea with High Morbidity and Mortality. N Engl J Med 353:2442–2449.

27. Phan JR. 2017. A Potential Solution to a Poopy Problem: Bile Salt Analogs as Prophylactics Against Clostridium Difficile Infection. Master's thesis. University of

Nevada, Las Vegas, NV.

28. Ramirez N, Liggins M, Abel-Santos E. 2010. Kinetic Evidence for the Presence of Putative Germination Receptors in Clostridium difficile Spores. J Bacteriol 192:4215–4222.

29. Shen A. 2015. A Gut Odyssey: The Impact of the Microbiota on Clostridium difficile Spore Formation and Germination. PLOS Pathog 11:e1005157.

30. Rupnik M, Wilcox MH, Gerding DN. 2009. Clostridium difficile infection: new developments in epidemiology and pathogenesis. Nat Rev Microbiol 7:526–536.

31. Otter JA, Yezli S, French GL. 2011. The Role Played by Contaminated Surfaces in the Transmission of Nosocomial Pathogens. Infect Control Hosp Epidemiol 32:687–699.

32. Eckstein BC, Adams DA, Eckstein EC, Rao A, Sethi AK, Yadavalli GK, Donskey CJ. 2007. Reduction of Clostridium Difficile and vancomycin-resistant Enterococcus contamination of environmental surfaces after an intervention to improve cleaning methods. BMC Infect Dis 7:61.

33. Gupta A, Khanna S. 2014. Community-acquired clostridium difficile infection: An increasing public health threat. Infect Drug Resist 7:63–72.

34. O'connor JR, Johnson S, Gerding DN. 2009. Clostridium difficile Infection Caused by the Epidemic BI/NAP1/027 Strain. Gastroenterology 136:1913–1924.

35. Khanna S, Pardi DS, Aronson SL, Kammer PP, Orenstein R, St Sauver JL, Scott Harmsen W, Zinsmeister AR. 2012. The Epidemiology of Community-acquired Clostridium difficile infection: A population-based study. Am J Gastroenterol 107:89–95.

36. Wilcox MH, Mooney L, Bendall R, Settle CD, Fawley WN. 2008. A case-control study of community-associated Clostridium difficile infection. J Antimicrob Chemother 62:388–396.

37. Louie TJ, Miller MA, Mullane KM, Weiss K, Lentnek A, Golan Y, Gorbach S, Sears P, Shue Y-K. 2011. Fidaxomicin versus Vancomycin for Clostridium difficile Infection. N Engl J Med 364:422–453.

38. Al-Nassir WN, Sethi AK, Nerandzic MM, Bobulsky GS, Jump RLP, Donskey CJ. 2008. Comparison of Clinical and Microbiological Response to Treatment of Clostridium difficile-Associated Disease with Metronidazole and Vancomycin. Clin Infect Dis 47:56–62.

39. Saha S, Kapoor S, Tariq R, Schuetz AN, Tosh PK, Pardi DS, Khanna S. 2019. Increasing antibiotic resistance in Clostridioides difficile: A systematic review and meta-analysis. Anaerobe 58:35–46.

40. Alexander F. 1929. On the Antibacterial Action of Cultures of a Penicillium, with Special Reference to Their Use in the Isolation of B. influenzae. Br J Exp Pathol 10:226–236.

41. Abraham EP, Chain E, Fletcher CM, Florey HW, Gardner AD, Heatley NG, Jennings MA. 1941. Further Observations on Penicillin. Lancet 2:177–189.

42. Kong K-F, Schneper L, Mathee K. 2010. Beta-lactam Antibiotics: From Antibiosis to Resistance and Bacteriology. APMIS 118:1-36.

43. Abraham EP, Newton GGF. 1961. The Structure of Cephalosporin C. Biochem J 79:377–393.

44. Poole K. 2004. Resistance to beta-lactam antibiotics. Cell Mol Life Sci 61:2200–2223.

45. Rolinson GN. 1979. 6-APA and the development of the ß-lactam antibiotics. J Antimicrob Chemother 5:7–14.

46. Palzkill T. 2013. Metallo-β-lactamase structure and function. Ann N Y Acad Sci 1277:91–104.

47. Cho H, Uehara T, Bernhardt TG. 2014. Beta-Lactam Antibiotics Induce a Lethal Malfunctioning of the Bacterial Cell Wall Synthesis Machinery. Cell 159:1300–1311.

48. Tipper DJ, Strominger JL. 1965. Mechanism of action of penicillins: a proposal based on their structural similarity to acyl-D-alanyl-D-alanine. Proc Natl Acad Sci 54:1133–1141.

49. Nicholas RA, Davies C. 2012. Structural Mechanisms of ß-Lactam Antibiotic Resistance in Penicillin-Binding Proteins, p. 397–425. *In* Dougherty, TJ, Pucci, MJ (eds.), Antibiotic Discovery and Development. Charleston, SC.

50. King DT, Solmaz S, Strynadka NCJ. 2017. The Mechanisms of Resistance to β-Lactam Antibiotics, p. 177–201. *In* Gotte, M, Berghuis, A, Matlashewski, G, Wainberg, MA, Sheppard, D (eds.), Handbook of Antimicrobial Resistance. New York.

51. Vollmer W, Blanot D, De Pedro MA. 2008. Peptidoglycan structure and architecture. FEMS Microbiol Rev 32:149–167.

52. Sauvage E, Kerff F, Terrak M, Ayala JA, Charlier P. 2008. The penicillin-binding proteins: structure and role in peptidoglycan biosynthesis. FEMS Microbiol Rev 32:234–258.

53. Sauvage E, Terrak M, Sauvage E, Terrak M. 2016. Glycosyltransferases and Transpeptidases/Penicillin-Binding Proteins: Valuable Targets for New Antibacterials. Antibiotics 5:12.

54. Peltier J, Courtin P, Meouche I El, Lemée L, Chapot-Chartier M-P, Pons J-L. 2011. Clostridium difficile Has an Original Peptidoglycan Structure with a High Level of N-Acetylglucosamine Deacetylation and Mainly 3-3 Cross-links. J Biol Chem 286:29053–29062.

55. Fisher JF, Mobashery S. 2016. ß-Lactam Resistance Mechanisms: Gram-Positive Bacteria and Mycobacterium tuberculosis. Cold Springs Harb Perspect Med 6:a025221.

56. Macheboeuf P, Contreras-Martel C, Job V, Dideberg O, Dessen A. 2006. Penicillin binding proteins: Key players in bacterial cell cycle and drug resistance processes. FEMS Microbiol Rev 30:673–691.

57. Peacock SJ, Paterson GK. 2015. Mechanisms of Methicillin Resistance in Staphylococcus aureus . Annu Rev Biochem 84:577–601.

58. Zapun A, Contreras-Martel C, Vernet T. 2008. Penicillin-binding proteins and β-lactam resistance. FEMS Microbiol Rev 32:361–385.

59. Calvez P, Breukink E, Roper DI, Dib L, Contreras-Martel C, Zapun A. 2017. Substitutions in PBP2b from-Lactam-resistant Streptococcus pneumoniae Have Different Effects on Enzymatic Activity and Drug Reactivity. J Biol Chem 292:2854–2865.

60. Otero LH, Rojas-Altuve A, Llarrull LI, Carrasco-López C, Kumarasiri M, Lastochkin E, Fishovitz J, Dawley M, Hesek D, Lee M, Johnson JW, Fisher JF, Chang M, Mobashery S, Hermoso JA. 2013. How allosteric control of Staphylococcus aureus penicillin binding protein 2a enables methicillin resistance and physiological function. PNAS 110:16808–16813.

61. Salernot AJ, Lampen J 0. 1986. Transcriptional Analysis of ß-Lactamase Regulation in Bacillus licheniformis. J Bacteriol 166:769–778.

62. Dumas J-L, Delden C, Perron K, KÃ¶hler T. 2006. Analysis of antibiotic resistance gene expression in *Pseudomonas aeruginosa* by quantitative real-time-PCR. FEMS Microbiol Lett 254:217–225.

63. Minami S, Yotsuji A, Inoue M, Mitsuhashi S. 1980. Induction of ß-Lactamase by Various ß-Lactam Antibiotics in Enterobacter cloacae. Antimicrob Agents Chemother 18:382–385.

64. Hanson ND. 1999. Regulation of Inducible AmpC Beta-Lactamase Expression Among Enterobacteriaceae. Curr Pharm Des 5:881–894.

65. Maddux MS. 1991. Effects of ß-Lactamase-Mediated Antimicrobial Resistance: The Role of ß-Lactamase Inhibitors. Pharmacother J Hum Pharmacol Drug Ther 11:40S-50S.

66. Blanco P, Hernando-Amado S, Reales-Calderon JA, Corona F, Lira F, Alcalde-Rico M, Bernardini A, Sanchez MB, Martinez JL. 2016. Bacterial Multidrug Efflux Pumps: Much More Than Antibiotic Resistance Determinants. Microorganisms 4:16.

67. Kaur P, Russell J. 1998. Biochemical coupling between the DrrA and DrrB proteins of the doxorubicin efflux pump of Streptomyces peucetius. J Biol Chem 273:17933–17939.

68. Steinfels E, Orelle C, Fantino J-R, Dalmas O, Rigaud J-L, Denizot F, Di Pietro A, Jault J-M. 2004. Characterization of YvcC (BmrA), a Multidrug ABC Transporter Constitutively Expressed in Bacillus subtilis. Biochemistry 43:7491–7502.

69. Collins B, Curtis N, Cotter PD, Hill C, Ross RP. 2010. The ABC transporter AnrAB contributes to the innate resistance of Listeria monocytogenes to nisin, bacitracin, and various β-lactam antibiotics. Antimicrob Agents Chemother 54:4416–4423.

70. Hürlimann LM, Corradi V, Hohl M, Bloemberg G V., Tieleman DP, Seeger MA. 2016. The heterodimeric ABC transporter EfrCD mediates multidrug efflux in Enterococcus faecalis. Antimicrob Agents Chemother 60:5400–5411.

71. Edric Orelle C, Mathieu K, Jault J-M. 2019. Multidrug ABC transporters in bacteria. Res Microbiol 170:381–391.

72. Dintner S, Staron´, AS, Berchtold E, Petri T, Mascher T, Gebhard S. 2011. Coevolution of

ABC Transporters and Two-Component Regulatory Systems as Resistance Modules against Antimicrobial Peptides in Firmicutes Bacteria †. J Bacteriol 193:3851–3862.

73. Meehl M, Herbert S, Götz F, Cheung A. 2007. Interaction of the GraRS two-component system with the VraFG ABC transporter to support vancomycin-intermediate resistance in Staphylococcus aureus. Antimicrob Agents Chemother 51:2679–2689.

74. Truong-Bolduc QC, Hooper DC. 2007. The transcriptional regulators NorG and MgrA modulate resistance to both quinolones and β-lactams in Staphylococcus aureus. J Bacteriol 189:2996–3005.

75. Mullany P, Allan E, Roberts AP. 2015. Mobile genetic elements in Clostridium difficile and their role in genome function. Res Microbiol 166:361–367.

76. Vuotto C, Moura I, Barbanti F, Donelli G, Spigaglia P. 2016. Subinhibitory concentrations of metronidazole increase biofilm formation in Clostridium difficile strains. FEMS Pathog Dis 74:ftv114.

77. Harnvoravongchai P, Pipatthana M, Chankhamhaengdecha S, Janvilisri T. 2017. Insights into drug resistance mechanisms in Clostridium difficile. Essays Biochem 61:81–88.

78. Britton RA, Young VB. 2014. Role of the Intestinal Microbiota in Resistance to Colonization by Clostridium difficle. Gastroenterology 146:1547–1553.

79. Chow AW, Cheng N, Bartlett KH. 1985. In Vitro Susceptibility of Clostridium difficile to New Beta-Lactam and Quinolone Antibiotics. Antimicrob Agents Chemother 28:842–844.

80. He M, Miyajima F, Roberts P, Ellison L, Pickard DJ, Martin MJ, Connor TR, Harris SR, Fairley D, Bamford KB, D'Arc S, Brazier J, Brown D, Coia JE, Douce G, Gerding D, Kim HJ, Koh TH, Kato H, Senoh M, Louie T, Michell S, Butt E, Peacock SJ, Brown NM, Riley T, Songer G, Wilcox M, Pirmohamed M, Kuijper E, Hawkey P, Wren BW, Dougan G, Parkhill J, Lawley TD. 2013. Emergence and global spread of epidemic healthcare-associated Clostridium difficile. Nat Genet 45:109–113.

81. Sandhu BK, Edwards AN, Anderson SE, Woods EC, McBride SM. 2020. Regulation and anaerobic function of the Clostridioides difficile β-lactamase. Antimicrob Agents Chemother 64:e01496-19.

82. Toth M, Stewart NK, Smith C, Vakulenko SB. 2018. Intrinsic Class D β-Lactamases of Clostridium difficile. MBio 9:e01803-18.

83. Ammam F, Meziane-cherif D, Mengin-Lecreulx D, Blanot D, Patin D, Boneca IG, Courvalin P, Lambert T, Candela T. 2013. The functional *vanG* $_{Cd}$ cluster of *Clostridium difficile* does not confer vancomycin resistance. Mol Microbiol 89:612–625.

84. Toth M, Tiago Antunes N, Stewart NK, Frase H, Bhattacharya M, Smith C, Vakulenko SB. 2015. Class D ß-lactamases do exist in Gram-positive bacteria. Nat Chem Biol 12:9–14.

85. Metcalf D, Sharif S, Weese JS. 2010. Evaluation of candidate reference genes in Clostridium difficile for gene expression normalization. Anaerobe 16:439–443.

86. Pfaffl MW. 2001. A new mathematical model for relative quantification in real-time RT-PCR. Nucleic Acids Res 29:2002–2007.

87. Kuan Ng Y, Ehsaan M, Philip S, Collery MM, Janoir C, Collignon A, Cartman ST, Minton NP. 2013. Expanding the Repertoire of Gene Tools for Precise Manipulation of the Clostridium difficile Genome: Allelic Exchange Using pyrE Alleles. PLoS One 8:e56051.

88. Gibson DG, Young L, Chuang R-Y, Venter JC, Hutchison CA, Smith HO. 2009. Enzymatic assembly of DNA molecules up to several hundred kilobases. Nat Methods 6:343–345.

89. Cartman ST, Minton NP. 2010. A mariner-Based Transposon System for In Vivo Random Mutagenesis of Clostridium difficile. Appl Environ Microbiol 76:1103–1109.

90. Ewing B, Green P. 1998. Base-calling of automated sequencer traces using phred. II. Error probabilities. Genome Res 8:186–194.

91. Hartman BJ, Tomasz A, Sabath L. 1984. Low-Affinity Penicillin-Binding Protein Associated with ß-Lactam Resistance in Staphylococcus aureus. J Bacteriol 158:513–516.

92. Hakenbeck R, Tarpay M, Tomasz A. 1980. Multiple Changes of Penicillin-Binding Proteins in Penicillin-Resistant Clinical Isolates of Streptococcus pneumoniae. Antimicrob Agents Chemother 17:364–371.

93. Moya B, Dötsch A, Juan C, Blázquez J, Zamorano L, Haussler S, Oliver A. 2009. β-Lactam Resistance Response Triggered by Inactivation of a Nonessential Penicillin-Binding Protein. PLoS Pathog 5:e1000353.

94. Peltier J, Courtin P, El Meouche I, Catel-Ferreira M, Chapot-Chartier MP, Lemée L, Pons JL. 2013. Genomic and expression analysis of the vanG-like gene cluster of Clostridium difficile. Microbiol (United Kingdom) 159:1510–1520.

95. Munita JM, Arias CA. 2016. Mechanisms of Antibiotic Resistance. Microbiol Spectr 4:2.

96. Lessard IAD. 2012. VanX D-,D-Dipeptidase, p. 1395–1400. *In* Rawlings, ND, Barrett, AJ, Woessner Jr., FJ (eds.), Handbook of Proteolytic Enzymes, 3rd ed. Elsevier Science & Technology.

97. Hamilton SM, Alexander JAN, Choo EJ, Basuino L, da Costa TM, Severin A, Chung M, Aedo S, Strynadka NCJ, Tomasz A, Chatterjee SS, Chambers HF. 2017. High-Level Resistance of Staphylococcus aureus to β-Lactam Antibiotics Mediated by Penicillin-Binding Protein 4 (PBP4). Antimicrob Agents Chemother 61:e02727-16.

98. Memmi G, Filipe SR, Pinho MG, Fu Z, Cheung A. 2008. Staphylococcus aureus PBP4 is essential for beta-lactam resistance in community-acquired methicillin-resistant strains. Antimicrob Agents Chemother 52:3955–66.

99. Peters K, Pazos M, Edoo Z, Hugonnet JE, Martorana AM, Polissi A, VanNieuwenhze MS, Arthur M, Vollmer W. 2018. Copper inhibits peptidoglycan LD-transpeptidases suppressing β-lactam resistance due to bypass of penicillin-binding proteins. Proc Natl Acad Sci U S A 115:10786–10791.

100. Sütterlin L, Edoo Z, Hugonnet J-E, Mainardi J-L, Arthur M. 2018. Peptidoglycan Cross-Linking Activity of L,D-Transpeptidases from Clostridium difficile and Inactivation of These Enzymes by β-Lactams. Antimicrob Agents Chemother 62:e01607-17.

101. Massova I, Mobashery S. 1998. Kinship and diversification of bacterial penicillin-binding proteins and β-lactamases. Antimicrob Agents Chemother 42:1–17.

102. Vuppada RK, Hansen CR, Strickland KAP, Kelly KM, McCleary WR. 2018. Phosphate signaling through alternate conformations of the PstSCAB phosphate transporter. BMC Microbiol 18:8.

103. Zea L, Prasad N, Levy SE, Stodieck L, Jones A, Shrestha S, Klaus D. 2016. A Molecular Genetic Basis Explaining Altered Bacterial Behavior in Space. PLoS One 11:e0164359.

104. Aunins TR, Erickson KE, Prasad N, Levy SE, Jones A, Shrestha S, Mastracchio R, Stodieck L, Klaus D, Zea L, Chatterjee A. 2018. Spaceflight Modifies Escherichia coli Gene Expression in Response to Antibiotic Exposure and Reveals Role of Oxidative Stress Response. Front Microbiol 9:310.

105. Emerson JE, Stabler RA, Wren BW, Fairweather NF. 2008. Microarray analysis of the transcriptional responses of Clostridium difficile to environmental and antibiotic stress. J Med Microbiol 57:757–764.

106. Greene NP, Kaplan E, Crow A, Koronakis V. 2018. Antibiotic resistance mediated by the MacB ABC transporter family: A structural and functional perspective. Front Microbiol 9:950.

107. Ngernsombat C, Sreesai S, Harnvoravongchai P, Chankhamhaengdecha S, Janvilisri T. 2017. CD2068 potentially mediates multidrug efflux in Clostridium difficile. Sci Rep 7:9982.

108. Cuenot E, Garcia-Garcia T, Douche T, Gorgette O, Courtin P, Denis-Quanquin S, Hoys S, Tremblay YDN, Matondo M, Chapot-Chartier M-P, Janoir C, Dupuy B, Candela T, Martin-Verstraete I. 2019. The Ser/Thr Kinase PrkC Participates in Cell Wall Homeostasis and Antimicrobial Resistance in Clostridium difficile. Infect Immun 87:e00005-19.

109. Lee EW, Huda MN, Kuroda T, Mizushima T, Tsuchiya T. 2003. EfrAB, an ABC Multidrug Efflux Pump in Enterococcus faecalis. Antimicrob Agents Chemother 47:3733–3738.

110. Dembek M, Barquist L, Boinett CJ, Cain AK, Mayho M, Lawley TD, Fairweather NF, Fagan RP. 2015. High-throughput analysis of gene essentiality and sporulation in Clostridium difficile. MBio 6:02383-14.

111. Van Opijnen T, Camilli A. 2013. Transposon insertion sequencing: a new tool for systems-level analysis of microorganisms. Nat Rev Microbiol 11:435–442.

CURRICULUM VITAE

Lara Turello
B.S. Biological Sciences
Email: turello.lara@gmail.com

EDUCATION

University of Nevada, Las Vegas

M.S. Biochemistry
Graduation: Spring 2020
GPA 4.0

B.S. in Biological Sciences, Cell and Molecular Biology concentration
Minor: Italian Studies
Graduation: Fall 2016
GPA 3.63

RESEARCH

University of Nevada, Las Vegas

Graduate Research Assistant in the Department of Chemistry and Biochemistry:
Worked under the direction of Dr. Ernesto Abel-Santos

Undergraduate Research in the School of Life Sciences:
Worked under the direction of Dr. Brian Hedlund
Worked under the direction of Dr. Penny Amy

United States Environmental Protection Agency's National Risk Management Research Laboratory, Cincinnati, Ohio:

Undergraduate intern:
Worked under the direction of Dr. Hodon Ryu

TEACHING

Organic Chemistry Lab I

CONFERENCES

- ASM Southern Nevada-Arizona Regional Conference
- ASM Southern Nevada-Arizona Regional Conference
- UNLV Undergraduate Research Showcase
- UNLV OUR Summer Undergraduate Research Symposium

PRESENTATIONS

- Turello, L., Abel-Santos, E. 2019. Putative cephalosporin resistance-associated gene expression in *Clostridium difficile* 630. ASM Southern Nevada-Arizona Regional Conference (Poster presentation)
- Turello, L. 2018. *Clostridium difficile* versus antibiotics: a battle using molecular weapons. Rebel Grad Slam (Oral presentation)

- Turello, L., Chan, L., Abel-Santos, E. 2018. Putative cephalosporin resistance-associated gene expression in *Clostridium difficile* 630. ASM Southern Nevada-Arizona Regional Conference (Poster presentation)
- Turello, L. 2016. Assessing the source of fecal contaminants in Las Vegas Valley urban watersheds. UNLV Research Week (Invited oral presentation)
- Turello, L. Friel, A., Hodon, R., Sarria, M. Gerrity, D., Menzel, N., Hedlund, B. 2016. Assessing the source of fecal contaminants in Las Vegas Valley urban watersheds. UNLV Undergraduate Research Showcase (Poster presentation)

SCHOLARSHIPS

- Alumni Association Scholarship
- Patricia Sastaunik Scholarship
- The College of Sciences' Excellence in Scholarship Award
- The Millennium Scholarship
- The Wolzinger Family Research Scholarship

AWARDS

- Outstanding Graduate for the Class of 2020
- First-Place winner at ASM Southern Nevada-Arizona Regional Conference for "Best Graduate Student Poster Presentation"
- 5th Annual Rebel Grad Slam Finalist
- First-Place winner at ASM Southern Nevada-Arizona Regional Conference for "Best Graduate Student Poster Presentation"
- Nevada's Women in STEM Honoree, awarded by Senator Jackie Rosen
- Second-Place winner at the Undergraduate Research Showcase in the Sciences, Health Sciences, and Engineering division
- "Outstanding Presentation Award" recipient at the UNLV OUR Summer Undergraduate Research Symposium
- Dean's Honor List

MEMBERSHIPS

- The UNLV Italian Club
- The American Society for Microbiology UNLV Student Chapter

VOLUNTEER WORK

- Treasurer for the ASM UNLV Student Chapter
- President of the UNLV Italian Club
- Active participant at the Boys and Girls Club through the ASM UNLV Student Chapter